Draft Final Report
For
The US EPA Region 10's 2004 Regional Geographic Initiative Grant:

Source Apportionment of Seattle and Portland Air Toxics and $PM_{2.5}$ Data

Chang-fu Wu[a,c], Timothy V. Larson[b], and L.-J. Sally Liu[c]
[a]College of Public Health, National Taiwan University, Taipei, Taiwan
[b]Department of Civil and Environmental Engineering, [c]Department of Environmental and Occupational Health Sciences, University of Washington

Prepared for John Williamson

Air Quality Program

Washington State Department of Ecology

FEBRUARY 9, 2006

EXECUTIVE SUMMARY

The National-scale Air Toxics Assessment (NATA) project is established by the US EPA to estimate potential health risks associated with the ambient concentrations of 32 urban air toxics and diesel particulate matters (DPM). As certain air toxics sources pose higher health risks than others, in order to develop effective control strategies to reduce population risks to air toxics, it is crucial to identify sources and the associated risks. Diesel exhaust (DE) is ubiquitous and long-term exposure to DE, in particular, is linked to exacerbation of existing allergies and asthma symptoms as well as elevated lung cancer risks. However, there is no available analytical method directly quantifying diesel particulate matter (DPM), which is a characteristic component for DE. This study utilizes source apportionment models and various datasets to identify sources of air toxics, with a special emphasis on DE and DPM.

Speciated $PM_{2.5}$ and air toxics measurements at the Beacon Hill (BH) and Georgetown (GT) in Seattle from 2000-2004 and at Roselawn (RL) in Portland site (RL) from 2002 were used for modeling. We applied the Positive Matrix Factorization (PMF) and Multilinear Engine (ME) for source apportionment analyses. The speciated $PM_{2.5}$ data were applied to these models with or without the addition of VOCs measurements to evaluate whether the addition of the VOCs data would provide additional finger prints for identifying the diesel source. For validating the source apportionment results, black carbon and PAHs measurements were compared with the apportioned DPM contributions. The source-specific risks were estimated as the sum of the products of the individual air

toxic concentration and its unit risk factor.

We found that at BH site, the source contribution estimates from the combined $PM_{2.5}$ and VOCs data gave a much better agreement between the PMF and ME models than that with the $PM_{2.5}$ data alone (Figure I). Secondary sulfate (~20%), vegetative burning (~30%), and diesel emissions (10%) are the largest three $PM_{2.5}$ sources. The predicted DPM correlated well with the BC measurements during both heating and non-heating seasons (R=0.71 and 0.77). However, BC is not a unique identifier for DPM. During the heating season vegetative burning $PM_{2.5}$ also correlated well with the BC measurements (R=0.83). Risk assessment results indicated that all sources, with the exception of 'marine', gave a sum of cancer risks greater than $1*10^{-6}$, with the highest risk from mobile sources.

At the GT site, due to the relatively small sample size, source apportionment findings were less consistent between the two models. At RL site, The PMF performs better than the ME model. It showed that the highest contributions to $PM_{2.5}$ are from vegetative burning (34%), secondary aerosols (32%), and gasoline emission (17%).

We concluded that with the combined speciated $PM_{2.5}$ and VOCs measurements, the source apportionment modeling results are more robust in identifying multiple sources of air toxics, particularly diesel and gasoline exhaust. This is supported by the evidence of a better agreement in source contribution estimates between PMF and ME models for the Beacon Hill datasets. Although the addition of VOCs measurements in the source apportionment analyses confirmed the stability of the diesel contribution estimates, it

significantly changed the gasoline contribution estimates from both PMF and ME models.

Vegetative burning and secondary sulfate are common and important contributing sources to $PM_{2.5}$ in both Seattle and Portland (Tables 3 and 5). The contribution estimates for diesel and gasoline vary among these three monitoring sites due to differences in the source mixture, number of sample size, and the availability of the VOCs data for source apportionment modeling (Tables 3-5).

We validated that DPM source estimates throughout the year agreed very well with the BC measurements (Figure 19a & b). We concluded that PMF and ME are both suitable for source apportionment based on our validation results, although PMF estimates agree slightly better with BC than those from ME. ME, however, provides more flexibility in modeling options than PMF. A slightly better agreement for the DPM estimates were obtained from the combined PM/VOC datasets as compared that from with the PM dataset alone. The vegetative burning source also agreed well with the BC measurements. Again, a better agreement was found when the combined PM/VOC datasets were used in the source apportionment modeling. Further validation of these source apportionment estimates should be performed using the air toxics release inventory data during the comparable time period for the areas of interest.

Figure I. Source contribution estimates at Beacon Hill.

(a) Source apportionment with speciated $PM_{2.5}$ data only

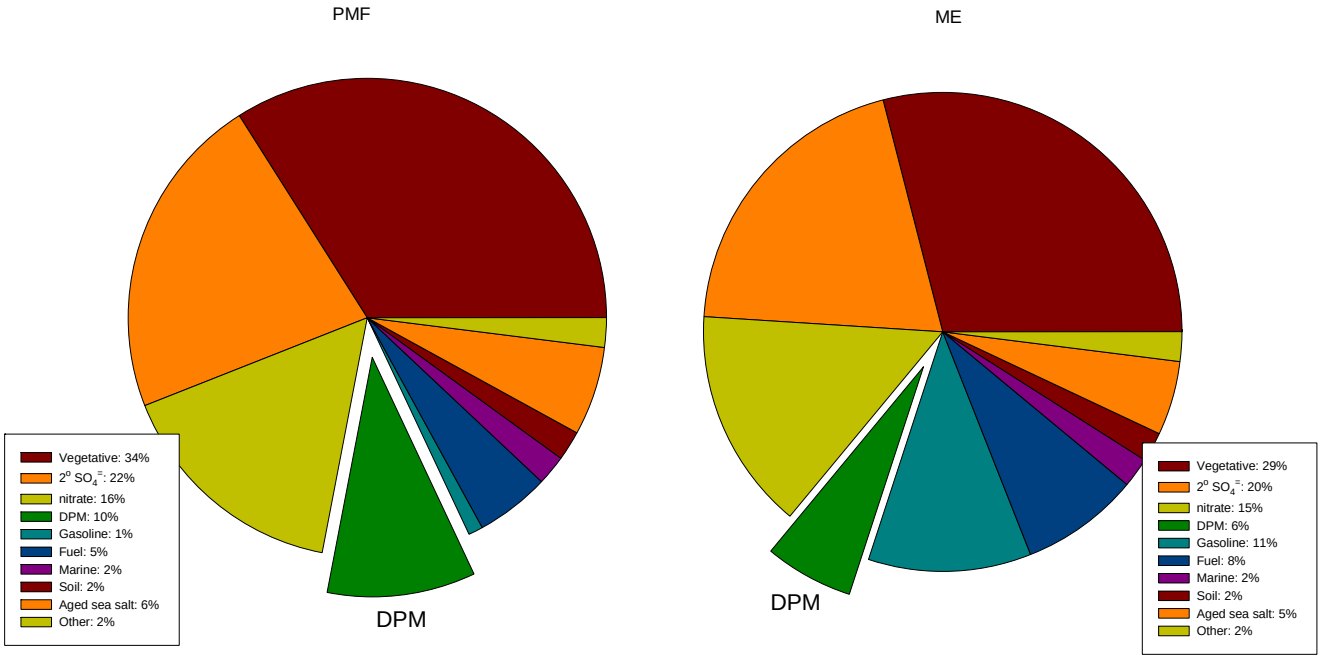

(b) Source apportionment with speciated $PM_{2.5}$ and VOC data combined

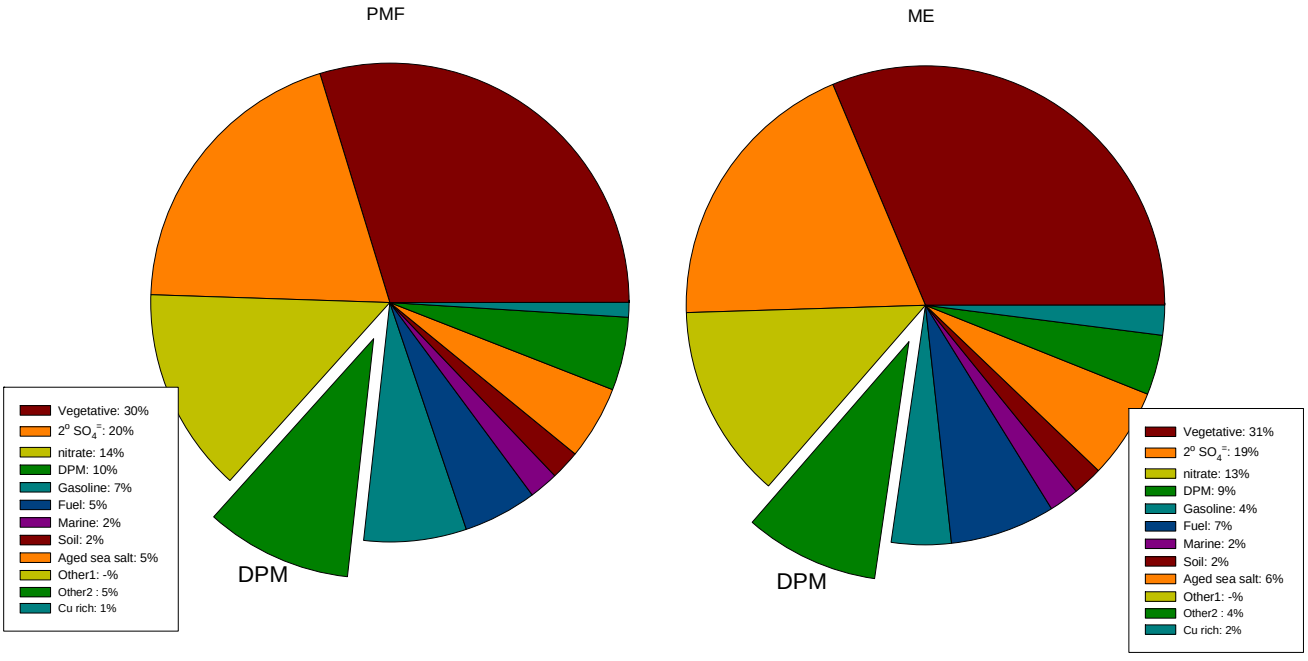

INTRODUCTION

The federal Clean Air Act Amendments of 1990 mandates the U.S. EPA to determine a subset of 188 urban hazardous air pollutants (HAPs) that potentially pose the greatest risks in urban areas, in terms of contribution to population health risk. The USEPA identified 33 urban HAPs in a 1995 ranking analysis (USEPA, 1999) and developed concurrent monitoring and modeling programs to evaluate potential exposures and risks to these top-ranked 33 HAPs. The National-scale Air Toxics Assessment (NATA) project is one of such programs that estimate potential cancer and non-cancer risks associated with the ambient concentrations of those toxics (USEPA, 2001). Results from the NATA project, which relies heavily on toxics inventories and dispersion modeling approaches, will be used to set priorities for the collection of additional air toxics data, including emissions data, ambient monitoring data, and information on adverse effects to health and the environment.

Risk estimates from the NATA modeling results often are used for developing control strategies to reduce population exposure to certain air toxics. However, for such control strategies to be cost-effective, identifying and quantifying specific sources and their contributions to the mixture of air toxics and thus risks in an urban is crucial. One solution is using the source apportionment modeling approach to distinguish sources. Most source apportionment studies aim at analyzing the origin of hazardous air pollutants (‘air toxics’) (Mukund et al., 1996; Jorquera and Rappengluck, 2004), while others focus on analyzing total fine particle mass. Only recently have researchers started to use source apportionment modeling to identify common sources (Harrison et al., 1996; Manoli et al., 2002; Schauer et al., 2002; Larsen and Baker, 2003). In the Pacific Northwest region,

source apportionment studies have been performed for $PM_{2.5}$ collected in Seattle (Larsen and Baker, 2003; Kim et al., 2004) and Spokane (Kim et al., 2002).

Among the air toxics sources commonly seen in the urban areas, diesel-engine exhaust (DE) is of special interest. The US EPA's diesel assessment report (USEPA, 2002) concluded that long-term exposure to DE is likely a lung cancer hazard. It also showed emerging evidence that DE exacerbates existing allergies and asthma symptoms. Although DE contains a complex mixture of gases and particulates, DE is most commonly characterized by measurements of diesel particulate matter (DPM) (USEPA, 2002). Currently there is no analytical method directly quantifying DPM. Ambient elemental carbon (EC) is commonly used to represent the portion of PM derived from DE; however, Schauer (2003) and others have demonstrated that EC is not a unique tracer for DPM. Studies applying source apportionment models to quantify DPM have indicated that a combination of particulate phase organic compounds (Chow and Watson, 2002), trace elements, and/or temperature resolved particulate carbon (Kim et al., 2003) are desired for such analyses. It has also been shown that source features for diesel and gasoline emissions differed in some VOCs (Schauer et al., 1999; Schauer, 2003) and polycyclic aromatic hydrocarbons (PAHs) (Harrison et al., 1996) contents. However, the EPA's $PM_{2.5}$ Speciation Trend Network (STN) does not routinely provide speciated organic compounds nor fully temperature resolved particulate carbon. This poses a challenge to apportion DPM using the STN measurements.

This project applied two different source apportionment models to a combination of air toxics and $PM_{2.5}$ speciation measurements to identify sources of the complex mixtures of

air pollutants in the two most populated cities in the northwest, Seattle, WA and Portland, OR. Our approach of combining air toxics and particulate pollutants in the source apportionment analysis was expected to enhance our ability to separate sources, especially for distinguishing DE from gasoline-engine exhaust. We also evaluate whether black carbon (BC) is a valid DPM surrogate by comparing the time-weighted BC data with the DPM concentration estimated by the source apportionment models. Another important part of this project is to calculate health risks based on the source apportionment results. Rather than quantifying health risk by air toxics as in most conventional risk assessment studies, we will calculate caner risk by each emission source.

METHODS

Sample collection and analysis

Speciated $PM_{2.5}$ and air toxics measurements at 2 monitoring sites in Seattle from 2000-2004 and at one Portland site from 2002 were used for modeling. In Seattle, air toxics and $PM_{2.5}$ have been monitored since 2000 at Beacon Hill (BH) and Georgetown (GT). The BH site is an urban-scale site and located in a highly populated neighborhood and reflects average $PM_{2.5}$ concentrations in a typical Seattle residential neighborhood (Goswami et al., 2002). It is impacted by a mix of urban sources including mobile and wood smoke. GT, a neighborhood-scale site, is located in the industrialized Duwamish River Valley and impacted by industrial, commercial and mobile sources, and reflects potentially maximum air toxics concentrations. In Portland, measurements from Roselawn (RL) were used. RL is an urban-scale site that is located in a highly populated

neighborhood near Interstate 5 and the Swan Island industrial area. RL represents conditions in a typical Portland residential neighborhood and is impacted by a mixture of urban sources including mobile and wood smoke.

The BH and RL sites are parts of the U.S. EPA Speciation Trends Network (STN) and the GT site follows similar protocols for $PM_{2.5}$ measurements. $PM_{2.5}$ samples were collected using samplers with Teflon, Nylon, and quartz filters, which were analyzed for $PM_{2.5}$ mass, elemental compositions, organic carbon (OC), elemental carbon (EC), sulfate (SO_4^{2-}), and nitrate (NO_3^-), respectively. Detailed description can be found in Kim et al. (2005). At BH and GT sites, formaldehyde and acetaldehyde were sampled with a DNPH cartridge and analyzed with HPLC-UV (EPA TO-11A method). VOCs, including Benzene,1,3-Butadiene, Carbon Tetrachloride, Chloroform, Dichloromethane, Tetrachloroethylene, and Trichloroethylene, were sampled with a SUMA canisters and analyzed with GC FID/ECD (EPA TO-14A method). In addition, an aethalometer was operated at the BH site to measure real-time black carbon since Feb, 2003. All data were obtained through the Washington Department of Ecology and Oregon Department of Environmental Quality.

Datasets

The datasets used for analysis were summarized in Table 1. We identified and quantified emissions sources by analyzing datasets A and B for Seattle and C for Portland. To determine whether the additional air toxics can help identify DPM, we analyzed sets A and B, with and without the VOCs and aldehydes measurements. Although gaseous air pollutants were also measured at the RL site, they were not included in the modeling data

because of the unavailability of the associated uncertainty values, which are required to run the source apportionment models. Due to the limited number of PAH data collected at BH, they were not included in the main sour apportionment modeling dataset. Instead, a linear regression modeling approach was used to estimate each source's contribution to individual PAH. To evaluate if BC can be a surrogate for DPM, we also compared the source contributions to the corresponding values of BC at BH.

Source apportionment models and their implementation

We applied the Positive Matrix Factorization (PMF) (Paatero, 1997) and Multilinear Engine (ME) (Paatero, 1999) for source apportionment analyses. Both methods are multivariate methods that solve a constrained bilinear mass balance model using an explicit least-squares equation. Both methods utilize similar object functions but with different minimization algorithms. The required input data include the mass concentrations and uncertainties of measured species. The main outputs are the source features and the reconstructed time series of source contributions. The input species concentrations and uncertainties were processed according to Polissar et al. (1998) and Kim et al. (2005). Namely, for concentrations below the MDL values, they were replaced by half of the MDL values and their uncertainties were set at 5/6 of the MDL values. Missing concentrations were replaced by the geometric mean concentrations and their uncertainties were set at five times this geometric mean concentration.

When both air toxics and $PM_{2.5}$ data were entered to the source apportionment model, the regression process calculates the rescaling factors for the obtained source features and contributions for each dataset separately. In our regression analyses, the measured $PM_{2.5}$

mass concentrations and the sum of the measured VOCs concentrations including aldehydes were used as the dependent variable for the $PM_{2.5}$ and air toxics portions, respectively.

Apportionment of PAHs

The stepwise linear regression model is used to estimate the contributions of various sources to each PAH:

$$PAH_j = \alpha_{io} + \sum \alpha_{ij} * Source_i \quad (1)$$

where PAH_j is the j^{th} PAH, $Source_i$ is the concentration of the i^{th} source estimated from the PMF or ME models, and $\alpha_{\iota\varphi}$ is the estimated regression coefficient. The value of *i* is determined with the stepwise regression algorithm, setting the significance level for entry into the model as 0.01. The source-specific concentration of each PAH is then determined as:

$$PAH_{ij} = \alpha_{ij} * Source_i \quad (2)$$

Where PAH_{ij} is the estimated concentration of the j^{th} PAH from the i^{th} source.

Risk assessment

Cancer risk (R) was calculated according to the basic equation presented below. Cancer risk attributable to inhalation exposure to each air toxics source is estimated as the sum of the products of individual air toxic exposure and its unit risk factor:

$$R_i = \sum Exposure_{ij} * UnitRisk_j \quad (3)$$

where R_i is the risk for the i^{th} source, $Exposure_{ij}$ is the concentration of the individual apportioned specie *j* from the i^{th} source, and $UnitRisk_j$ is the incremental increase in risk per $\mu g/m^3$ increase in exposure concentration for the j^{th} specie. Unit risk factors were extracted from databases provided by IRIS (Integrated Risk Information System), NATA and CalEPA (California Environmental Protection Agency).

The source-specific cancer risk of PAHs is estimated by calculating the benzeo(a)pyrene (BaP) equivalent concentration (BaP_{eq}) first, which is the product of each PAH's concentration for the source of interest (PAH_{ij} in Eq 2) and its toxicity equivalency factor (TEF). The TEF is an estimate of the relative toxicity compared to BaP and is obtained from the US EPA. Cancer risk from exposures to PAH attributable to each air toxics source is estimated as:

$$R_{PAH,i} = \sum BaP_{eq,i,j} * UnitRisk_{BaP} \qquad (4)$$

where $BaP_{eq,i,j}$ is the BaP_{eq} of the j^{th} PAH associated with the i^{th} source, and the $UnitRisk_{BaP}$ is the unit risk for BaP (1.1×10^{-6} /ng/m^3, CalEPA).

For DPM, the Cal EPA suggested a unit risk of $3*10^{-4}$ /$\mu g/m^3$ (CalEPA, 2005). Thus, in addition to using Eq (3), the DPM associated cancer risk is also calculated as the product of this unit risk and the DPM concentration estimated from the source apportionment model. In the NATA project, EPA estimated population's exposures to DPM using air dispersion models with emission inventory and meteorological data. The spatial resolution of the estimated concentrations is at the census tract level. We retrieved the NATA-estimated DPM concentration and calculate the cancer risk with the Cal EPA's unit

risk estimate. We further calculated the mean values of the NATA-DPM concentrations at those census tracts falling within certain radius (i.e. 1 km, 3 km, and 5 km) from the monitoring sites. The DPM related cancer risks estimated from various approaches were then compared with each other.

RESULTS

Quality control

Concentrations of formaldehyde from 2003/7/8 to 2003/8/25 at BH were identified to be almost 10 times higher than the rest of the measurements. In the 2004 Air Quality Data Summary Report (PSCAA, 2005) from the Puget Sound Clean Air Agency, it was stated that a local formaldehyde source, including solvents that are sometimes used in research projects, was possibly present at the BH site during this period. The academic community occasionally uses the BH site for researches. Although it is not known at this time if this is what caused a significant increase in concentrations, they concluded that it is unlikely of having a regional increase of formaldehyde during this time. These measurements were removed from the dataset.

Table 2 summarizes the concentrations of $PM_{2.5}$ species and VOCs as well as their MDL's, used in the source apportionment models. At the BH, URG sampler was used and PM species were included in this study only when at least 30% of the values are above the MDL. Important PM species including Ca, Cl, Cu, EC, Fe, Pb, Ni, Na, Se, Si, sulfate, S, Va, and Zn are mostly above the MDL. Note that most VOC measurements are above the MDL as well. Uncertainty value for individual $PM_{2.5}$ sample was not reported prior to

2003 in the STN. Kim et al. (Kim et al.) examined a limited set of measured concentrations in the STN and their associated uncertainties. They derived a comprehensive set of error structures and uncertainty values that could be used for source apportionment studies of STN data. The uncertainty values for the speciated $PM_{2.5}$ samples at BH based on the information given in Kim et al. (Kim et al.) were then calculated and applied in this study. As for GT site, from 2000/4 to 2002/5 the URG sampler was used and after 2002/6 the Andersen sampler took the place of URG sampler. The MDL for each sampler was shown in Table 2. As at the BH site, the uncertainty values calculated from information given in Kim et al. (Kim et al.) was applied. At the RL site, the MDL and uncertainty values from 2002/10 to 2003/7 were not available. After 2003/7, individual MDL and uncertainty values were given (Table 2). In order to keep data consistency, we used the MDL and uncertainty values given in Kim et al. (Kim et al.) for the modeling work at the RL site.

Kim et al. (Kim et al.) also reported that the particulate OC concentrations measured by the STN samplers are not blank corrected and there exists a positive artifact in the OC concentrations. Thus, following their suggestion, we utilized the intercept of the regression model for OC concentration against $PM_{2.5}$, and estimated the blank concentrations to be 268 ng/m^3 for BH and 586 ng/m^3 for RL (Figures 1 and 2). These estimated blank values were consequently subtracted from all measured OC concentrations at the two sites respectively. Note that such phenomenon was not observed at the GT site (intercept=-161.3 ng/m^3, p=0.2) and OC concentrations at this site were not adjusted.

Source apportionment at Beacon Hill

Figures 3 and 5 show the source features derived from PMF and ME models, respectively, using the speciated $PM_{2.5}$ data only. The associated source contribution estimates (SCE) between heating/non-heating seasons and weekend/weekday are shown in Figures 4 and 6. The vegetative burning PM was characterized by the high levels of OC, EC and K with relatively low concentrations in other trace elements. The SCE also was higher at the heating season than at the non-heating season due to the more frequent burning activities in the winter. The soil source was distinguished by the characteristically richness in crustal-derived materials such as Si and Ca. The marine source was identified by the high levels of Cl and Na. Secondary sulfate and nitrate rich sources were clearly marked by the high concentrations of sulfate and nitrate, respectively. Because the secondary sulfate source is the result of photochemical activity, the contribution in summer is apparently higher in winter. On the contrary, nitrate rich aerosol tends to form in the season with low temperature and high humidity, therefore, the season variation of relative high contribution in winter can be observed (Kim et al., 2004). The fuel source was characterized by its high proportion of V and Ni. Although diesel and gasoline sources have similar carbon fractions, it is easy to separate diesel source by its high levels of Mn and Fe. Moreover, the weekday/weekend variation of diesel and gasoline happened to agree the traffic peak on weekday. Aged sea salt is identified by its high mass fractions of sulfate, nitrate, Na, and K. Since it is correlated with photochemical activity, the slightly season variation with higher contribution in summer was observed. The ‘other1’ feature is probably a combination of some local sources such as the paper mill and ferrous metal (Kim et al., 2005). These two models generally produced similar features.

The SCE for each source are shown in Table 3. Vegetative burning, secondary sulfate, nitrate rich sources were the most abundant contributors at BH region. The SCE agreement between the model was especially good for secondary sulfate, nitrate rich, marine, soil, aged sea salt and other1 sources. However, the PMF and ME models estimated that the SCE of gasoline was 1% and 11%, respectively.

Figures 7 and 9 show the source features derived from PMF and ME models, respectively, using the combined speciated $PM_{2.5}$ and VOCs data. The SCE between heating/non-heating seasons and weekend/weekday are shown in Figures 8 and 10. Most source features were still similar between the PMF and ME estimates. Nevertheless, with the addition of VOCs data, another unknown source was derived. The Other2 and Cu rich are probably derivation of the Other1 in Figures 3 and 5. Their features are rich in the elements that also were abundant in Other1. The SCE had a much better agreement between these two models for all the sources (Table 3), compared to using only the speciated $PM_{2.5}$ data only. For gasoline, the PMF and ME models estimated that the SCE was 7% and 4%, respectively.

It was originally expected that the VOCs features derived from the models should also provide information for identifying different sources. The secondary aerosol sources were rich in acetaldehyde and formaldehyde. The traffic relative sources generally had high percentage of acetaldehyde, formaldehyde, and benzene. However, the VOCs measured in this study overlapped in these traffic related features and thus may not be unique tracers. Several studies showed that acetaldehyde and formaldehyde are higher in not only gasoline but also diesel exhaust. The proportions of many VOCs in diesel and

gasoline did not have good agreement among different studies (Kirchstetter et al., 1996; Schauer et al., 1999; Siegl et al., 1999; Grosjean et al., 2001; Ho et al., 2002)

When comparing SCE between the datasets within the PMF models, the addition of VOCs data to the PM species resulted in comparable SCE for vegetative burning, secondary sulfate, nitrate, diesel, fuel, marine, soil and aged sea salt, while stark differences in SCE were observed for gasoline sources (Table 3). As for ME source contribution estimates, the same comparable results were also observed with and without the addition of the VOCs data. For VOCs source contribution estimates, both models identified gasoline as a major contributing source with diesel exhaust as the second largest contributor (Table 3, last 4 columns).

The source feature for diesel exhaust is readily identified with or without the inclusion of the VOCs data, as there is always one source feature having high EC, OC, Fe and Mn, and with higher concentrations during weekdays than weekends. This is probably due to the high impact of DPM at the BH site thus resulting in the unique abundance of EC, OC, Fe, and Mn in the diesel source feature. BH is surrounded by two major highways, I5 and I90, and could be under the influence of diesel exhaust from the marine sources in the Puget Sound, approximately 5 miles way. The SCE are similar (6%~10%), regardless of the inclusion of the VOCs data or the source apportionment algorithms (Table 3). Thus, for diesel SCE, the addition of the VOCs measurements did not clearly result in a significant difference in source contribution estimates.

Source apportionment at Georgetown

Figures 11 and 12 show the sources features at the GT site from the PMF and ME model, respectively, using the speciated $PM_{2.5}$ data only. The SCE are shown in Table 4. With less than 50% of the data points (n=133) as compared with those at the BH site (n=277), only three common source features were identified from both models: vegetative burning, secondary sulfate, and marine. The PMF model identified two additional features (other sources 1 and 2 in Figure 11); both are rich in Fe, Mn, OC, EC and higher on weekdays than weekends (data not shown). These two sources probably are diesel and gasoline. However, we were unable to distinguish between these two sources. The ME model identified three additional sources based on the feature signatures: diesel, gasoline, and soil (Figure 12). Nevertheless, the SCE of diesel at GT (3%, Table 4) was smaller than that at BH. GT is located at the bottom of the Duwamish Valley while BH is on a ridge. Under stable conditions, the average concentrations at the valley floor are expected to be higher than at the ridge for pollutants emitted near the ground (e.g. mobile). This suggests that the diesel source for the GT dataset was not separated completely from other sources.

Results derived from PMF and ME models using both speciated $PM_{2.5}$ and VOCs data are shown in Figures 13 and 14, respectively. Compared with the features derived from using only speciated $PM_{2.5}$ data (Figures 11 and 12), adding VOC data enhanced our ability to identify source features in this case. Both PMF and ME models identified vegetative burning, secondary sulfate, diesel, gasoline, and marine sources. ME model identified one additional soil source. The SCE from both models are shown in Table 4. Generally, the agreement between the two models' estimates dose not seem to be as good as the agreement found in BH site (Table 3). This is because we have much less data (N=133) in GT, which suggests that our modeling results may not be robust enough to make

conclusive assessment.

We also ran the PMF and ME models by combining the BH and GT data. However, this approach failed to resolve source successfully, probably due to different sources influencing one but not the other site.

Source apportionment at Roselawn

Figures 15 and 17 show the source features obtained through PMF and ME, respectively, with PM species data only at the RL site. The SCE values were summarized in Table 5 and the SCE between heating/non-heating seasons and weekend/weekday are shown in Figures 16 and 18. From the PMF modeling results, we identify nine sources with an unknown feature rich in Zn, which probably came from certain local emission sources. Compared to the results at BH, some sources were not separated clearly at RL. The fuel and gasoline sources were hard to be differentiated since they were both rich in OC and EC. With the presumption of higher contribution from gasoline and fuel, we labeled the two features accordingly. Still, it seems that the PMF model performs better than the ME model. The ME model separated only six sources. It did not further separate the secondary aerosol into the secondary sulfate and nitrate rich sources. Moreover, the feature labeled as soil may be actually a combination of gasoline and soil sources.

Both PMF and ME models indicated that vegetative burning and secondary aerosol sources were the major emission sources at RL (Table 5). The vegetative burning and soil source contributions were higher in ME model, probably because of the gasoline feature were not separated clearly in the ME model. This also suggests that the SCE for the DPM

from the PMF model (7%) should be more accurate than the one from the ME model (4%).

Diesel particulate matters & Black Carbon

Figure 19 showed the scatter plots of the daily time-averaged BC measurements at the BH site versus the DPM and vegetative burning particle concentrations estimated from both PMF and ME models, using the combined speciated $PM_{2.5}$ and VOC data. Regardless of the seasons, BC correlated well with the DPM source (r=0.83). BC and vegetative burning PM also correlated well during the heating season (Oct-Feb), with an r of 0.85. Relationships between BC and DPM estimated from PMF and ME models with $PM_{2.5}$ data only are shown in Figure 20. For BC vs. DPM, the r is 0.70 during the heating season and 0.77 during the non-heating season. These values were slightly lower than the r values when the combined speciated $PM_{2.5}$ and VOCs datasets were used in modeling. Similar results were observed for vegetative burning PM vs. BC during the heating season, i.e., r=0.83 (PM only) vs. 0.85 (PM+VOCs). This indicated that BC is not a unique tracer for DPM, as it correlated well with both DPM and vegetative burning particles. It also indicated that results from the source modeling using the combined $PM_{2.5}$ and VOC datasets may give better estimates than those from $PM_{2.5}$ only.

Judging from the fact that (1) the SCE had a much better agreement between the PMF and ME models when using the speciated $PM_{2.5}$ and VOCs datasets and (2) applying PMF model with the combined speciated $PM_{2.5}$ and VOCs datasets revealed the best correlation with BC concentrations, the following PAH and risk assessment analyses were conducted with the PMF model using the combined speciated $PM_{2.5}$ and VOCs

datasets.

PAH analysis

The PAHs data collected at BH had a small sample size (N=19~57). It is impractical to put those measurements into the source apportionment models. We instead applied a linear regression modeling approach to apportion the PAHs (Eqs 1 and 2). The source-specific concentrations in the equations were estimated from the PMF model with the combined speciated $PM_{2.5}$ and VOC data. The results showed that negative coefficients were presented in some sources, due to the medium correlation between some sources (Table 6). The negative regression coefficient was most apparent for DPM and gasoline particles. The correlation coefficient between the two sources is 0.40 (Table 6). A new mobile source which was the sum of gasoline and diesel particles was then created to avoid having negative regression coefficients.

Table 7 showed the stepwise regression results when setting the selection criterion of $r<0.01$. Only the mobile, fuel, and soil sources were selected in the final model. The estimated PAHs concentrations from each source (Eq 2) were shown in Table 8. It can be seen that the sum of the estimated source-specific PAHs concentrations were lower than the measured concentrations. This is because the intercept, which represents the contribution from other unidentified sources, is not included in the summation calculation.

Risk assessment

The risk characterization was conducted at the BH using source-specific concentrations

estimated from the PMF model with the combined speciated $PM_{2.5}$ and VOC data. The unit risks of metals and VOCs (Eq 3) and TEF of PAHs used for the risk calculations are shown in Tables 9 and 10, respectively. The estimated excessive cancer risks for each source by pollutants are summarized in Table 11. It was found that the risks attributed to PAHs were relatively small ($< 10^{-9}$), while most of the risks were associated with the $PM_{2.5}$ and VOCs. All sources except 'marine' gave a sum of cancer risks higher than $1*10^{-6}$, with the highest risk from mobile sources.

While focusing on the DPM, the risk estimated from the specie-by-specie approach is apparently lower than the ones from other approaches (Figures 21 and 22). This is probably because we only have 4 metal species for the $PM_{2.5}$. This risk is still low ($6*10^{-6}$) after adding the risks from the DPM associated VOCs. Applying the approaches of using the DPM unit risk from the CalEPA, the risks estimates are in the same magnitude ($2.35 * 10^{-4}$ to $6.52 *10^{-4}$). Note that the EPA stated that the results from the NATA study are most meaningful when viewed at the State or national level.

CONCLUSIONS

We concluded that with the combined speciated $PM_{2.5}$ and VOCs measurements, the source apportionment modeling results are more robust in identifying multiple sources of air toxics, particularly diesel and gasoline exhaust. This is supported with the evidence of a better agreement in source contribution estimates between PMF and ME models for the Beacon Hill datasets. Although the addition of VOCs measurements in the source apportionment analyses confirmed the stability of the diesel contribution estimates, it significantly changed the gasoline contribution estimates from both PMF and ME

models.

The source features differ among these 3 monitoring sites (BH, GT, and RL) due to various source mixtures. Vegetative burning and secondary sulfate are common and important contributing sources to $PM_{2.5}$ in both Seattle and Portland. The contribution estimates for diesel and gasoline vary among these three monitoring sites due to differences in the source mixture, number of sample size, and the availability of the VOCs data for source apportionment modeling.

As these source apportionment results have not been validated with estimates from the air toxics release inventory, measurements of BC as a surrogate for diesel exhaust could not be conclusively validated. We used the BC measurements instead as a means of across-checking the diesel and vegetative burning contribution estimates. BC agreed very well with DPM throughout the year, with a better agreement for estimates obtained from the combined PM/VOC datasets. BC agreed equally well with the vegetative burning source, again with a better agreement with the combined PM/VOC datasets were utilized in the source apportionment modeling.

All sources except ‘marine’ gave a sum of cancer risks higher than $1*10^{-6}$ at the BH site, with the highest risk from mobile sources. Most of the risks were associated with the $PM_{2.5}$ and VOCs, rather than the PAH. It was also found that for the DPM the risk estimate from the specie-by-specie approach is much lower than the ones from using the unit-risk approach.

Further validation of these source apportionment estimates should be performed using the air toxics release inventory data during the comparable time period for the areas of interest.

REFERENCES

CalEPA, 2005. http://www.arb.ca.gov/toxics/dieseltac/de-fnds.htm 2005/12/19

Chow, J. C. and Watson, J. G., 2002. Review of Pm2.5 and Pm10 Apportionment for Fossil Fuel Combustion and Other Sources by the Chemical Mass Balance Receptor Model. Energy & Fuels 16(2), 222-260.

Goswami, E., Larson, T., Lumley, T. and Liu, L. J. S., 2002. Spatial Characteristics of Fine Particulate Matter: Identifying Representative Monitoring Locations in Seattle, Washington. Journal Of The Air & Waste Management Association 52(3), 324-333.

Grosjean, D., Grosjean, E. and Gertler, A. W., 2001. On-Road Emissions of Carbonyls from Light-Duty and Heavy-Duty Vehicles. Environmental Science & Technology 35(1), 45-53.

Harrison, R. M., Smith, D. J. T. and Luhana, L., 1996. Source Apportionment of Atmospheric Polycyclic Aromatic Hydrocarbons Collected from an Urban Location in Birmingham, Uk. Environmental Science & Technology 30(3), 825-832.

Ho, K. F., Lee, S. C. and Chiu, G. M. Y., 2002. Characterization of Selected Volatile Organic Compounds, Polycyclic Aromatic Hydrocarbons and Carbonyl Compounds at a Roadside Monitoring Station. Atmospheric Environment 36(1), 57-65.

Jorquera, H. and Rappengluck, B., 2004. Receptor Modeling of Ambient Voc at Santiago, Chile. Atmospheric Environment 38(25), 4243-4263.

Kim, E., Larson, T. V., Hopke, P. K., Slaughter, C., Sheppard, L. E., et al., 2002. Source Identification of Pm2.5 in an Arid Northwest U.S. City by Positive Matrix Factorization. Atmospheric Research submitted.

Kim, E., Hopke, P. K., E. and S., E., 2003. Improving Source Identification of Atlanta Aerosol Using Temperature Resolved Carbon Fractions in Positive Matrix Factorization. Aerosol Science and Technology sumbitted.

Kim, E., Hopke, P. K. and Edgerton, E. S., 2004. Improving Source Identification of Atlanta Aerosol Using Temperature Resolved Carbon Fractions in Positive Matrix

Factorization. Atmospheric Environment 38(20), 3349-3362.

Kim, E., Hopke, P. K., Larson, T. V., Maykut, N. N. and Lewtas, J., 2004. Factor Analysis of Seattle Fine Particles. Aerosol Science And Technology 38(7), 724-738.

Kim, E., Hopke, P. K. and Qin, Y. J., 2005. Estimation of Organic Carbon Blank Values and Error Structures of the Speciation Trends Network Data for Source Apportionment. Journal Of The Air & Waste Management Association 55(8), 1190-1199.

Kirchstetter, T. W., Singer, B. C., Harley, R. A., Kendall, G. B. and Chan, W., 1996. Impact of Oxygenated Gasoline Use on California Light-Duty Vehicle Emissions. Environmental Science & Technology 30(2), 661-670.

Larsen, R. K. and Baker, J. E., 2003. Source Apportionment of Polycyclic Aromatic Hydrocarbons in the Urban Atmosphere: A Comparison of Three Methods. Environmental Science & Technology 37(9), 1873-1881.

Manoli, E., Voutsa, D. and Samara, C., 2002. Chemical Characterization and Source Identification/Apportionment of Fine and Coarse Air Particles in Thessaloniki, Greece. Atmospheric Environment 36(6), 949-961.

Mukund, R., Kelly, T. J. and Spicer, C. W., 1996. Source Attribution of Ambient Air Toxic and Other Vocs in Columbus, Ohio. Atmospheric Environment 30(20), 3457-3470.

Paatero, P., 1997. A Weighted Non-Negative Least Squares Algorithm for Three-Way 'Parafac' Factor Analysis. Chemometrics And Intelligent Laboratory Systems 38(2), 223-242.

Paatero, P., 1999. The Multilinear Engine - a Table-Driven, Least Squares Program for Solving Multilinear Problems, Including the N-Way Parallel Factor Analysis Model. Journal Of Computational And Graphical Statistics 8(4), 854-888.

Polissar, A. V., Hopke, P. K. and Paatero, P., 1998. Atmospheric Aerosol over Alaska - 2. Elemental Composition and Sources. Journal Of Geophysical Research-Atmospheres 103(D15), 19045-19057.

PSCAA, 2005. 2004 Air Quality Data Summary. Pudget Sound Clear Air Agency.

Schauer, J. J., Kleeman, M. J., Cass, G. R. and Simoneit, B. R. T., 1999. Measurement of

Emissions from Air Pollution Sources. 2. C-1 through C-30 Organic Compounds from Medium Duty Diesel Trucks. Environmental Science & Technology 33(10), 1578-1587.

Schauer, J. J., Fraser, M. P., Cass, G. R. and Simoneit, B. R. T., 2002. Source Reconciliation of Atmospheric Gas-Phase and Particle-Phase Pollutants During a Severe Photochemical Smog Episode. Environmental Science & Technology 36(17), 3806-3814.

Schauer, J. J., 2003. Evaluation of Elemental Carbon as a Marker for Diesel Particulate Matter. Journal Of Exposure Analysis And Environmental Epidemiology 13(6), 443-453.

Siegl, W. O., Hammerle, R. H., Herrmann, H. M., Wenclawiak, B. W. and Luers-Jongen, B., 1999. Organic Emissions Profile for a Light-Duty Diesel Vehicle. Atmospheric Environment 33(5), 797-805.

USEPA, 1993. Provisional Guidance for Quantitative Risk Assessment of Ploycyclic Aromatic Hydrocarbons. US Environmental Protection Agency, Research Triangle Park, NC EPA-600/R-93/089.

USEPA, 1999. National Air Toxics Program: The Integrated Urban Strategy. Federal Register 64 (137), FRL–6376–6377.

USEPA, 2001. National-Scale Air Toxics Assessment for 1996 (Draft). EPA-453/R-01-003.

USEPA, 2002. Health Assessment Document for Diesel Engine Exhaust. Washington, Dc, National Center for Environmental Assessment.

Table 1. Datasets used in source apportionment from the Beacon Hill (BH), Georgetown (GT), and Roselawn (RL) sites.

Dataset	Location	Air monitoring data	Period
A	BH	speciated PM2.5,VOCs, aldehydes, (PAHs, BC)*	2000.2 -2004.12
B	GT	speciated PM2.5, VOCs, aldehydes	2000.5 -2003.2
C	RL	speciated PM2.5	2002.10-2004.12

* Available but not included in the main source apportionment models due to the limited sample size.

Table 2. Average concentration of PM species and VOCs used for source apportionment modeling at (a) the BH and GT sites and (b) the RL site.

		BH(n=268)			GT(n=133)			
element	abbrev	mean	MDL(URG)	BDL	mean	MDL(URG)	MDL(Anderson)	BDL
Aluminum	Al				17.9	4.36	4.36	44.40%
Ammonium	NH4	456.09	7	0.00%	516.73	7	15	1.50%
Arsenic	As	0.97	0.99	60.07%	1.57	0.99	0.99	41.40%
Barium	Ba				18.96	23.6	23.6	61.70%
Bromine	Br	2.03	0.8	11.94%	3.64	0.8	0.8	7.50%
Calcium	Ca	26.74	1.39	0.00%	50.61	1.39	1.39	0.00%
Chlorine	Cl	60.20	2.32	34.33%	105.65	2.32	2.32	17.30%
Chromium	Cr	1.58	0.63	27.99%	3.51	0.63	0.63	18.80%
Copper	Cu	4.30	0.54	5.22%	8.22	0.54	0.54	3.00%
Elemental Carbon	EC	612.94	59	1.12%	1068	59	137	0.00%
Iron	Fe	51.64	0.79	0.00%	160.97	0.79	0.79	0.00%
Lead	Pb	3.74	2.2	27.61%	9.82	2.2	2.2	9.80%
Magnesium	Mg				11.29	7.38	7.38	60.20%
Manganese	Mn	3.02	0.92	30.22%	13.93	0.92	0.92	11.30%
Molybdenum	Mo				2.73	1.91	1.91	58.60%
Nickel	Ni	2.25	0.5	22.01%	4.21	0.5	0.5	13.50%
Nitrate Nonvolatile	NO3	459.27	3	0.00%				
Organic carbon	OC	2561.91	59	1.12%	4327.65	59	134	0.00%
Potassium Ion	K	29.45	6	42.54%	44.19	6	13	29.30%
Silicon	Si	42.07	3.02	2.99%	69.54	3.02	3.02	0.00%
Sodium Ion	Na	151.82	12	2.24%	219.43	12	28	0.00%
Sulfate	SO4	1191.15	5	0.00%	1462	5	11	0.00%
Tin	Sn	5.10	7.17	66.04%	6.81	7.17	7.17	49.60%
Titanium	Ti	2.63	0.83	21.64%	5.67	0.83	0.83	3.00%
Vanadium	V	3.47	0.6	23.51%	4.81	0.6	0.6	15.00%
Zinc	Zn	8.80	0.58	0.00%	24	0.58	0.58	0.00%
Acetaldehyde	Ace	1448.42	98.97	3.73%	1404.87	98.98		9.00%
Formaldehyde	For	1505.76	95.71	4.10%	1913.91	95.71		9.00%
Benzene	Ben	1329.72	44.66	0.37%	2080.61	44.66		0.00%
1,3-Butadiene	But	119.10	46.38	22.39%	214.6	46.38		15.80%
Chloroform	Chl	237.84	48.26	0.75%	143.18	48.26		1.50%
Carbon tetrachloride	Car	641.24	31.08	0.37%	653.7	31.08		0.80%
Tetrachloroethylene	Tet	182.37	33.54	3.36%	369.57	33.54		1.50%
Trichloroethylene	Tri	169.18	53.17	14.55%	479.51	53.17		1.50%

(b) RL site.

Element	abbrev	2002.10~2003.7[(1)]				2003.7-2004.12[(2)]			
		mean	MDL[(1)]	UNC[(1)]	BDL	mean	MDL[(2)]	UNC[(2)]	BDL
Ammonium	NH_4	643.68	17.00	0.070	9.88%	581.48	16.52	0.041	0.00%
Arsenic	As	2.15	2.47	0.200	62.96%	2.47	2.46	0.001	59.65%
Bromine	Br	1.80	1.99	0.050	59.26%	1.68	1.95	0.001	54.39%
Calcium	Ca	33.79	3.47	0.110	0.00%	43.22	6.31	0.004	1.75%
Chlorine	Cl	22.67	5.78	0.100	45.68%	68.49	9.42	0.008	34.50%
Chromium	Cr	2.10	1.59	0.050	59.26%	2.04	2.07	0.001	61.99%
Copper	Cu	6.75	1.35	0.050	17.28%	9.70	2.29	0.001	22.22%
Elemental carbon	EC	908.70	146.00	0.070	2.47%	728.78	240.06	0.282	7.02%
Iron	Fe	74.14	1.96	0.050	0.00%	94.31	2.36	0.006	2.34%
Lead	Pb	8.06	5.49	0.050	41.98%	6.50	5.22	0.002	49.71%
Manganese	Mn	10.13	2.31	0.050	44.44%	8.03	2.22	0.001	34.50%
Nickel	Ni	1.90	1.25	0.050	38.27%	1.88	1.72	0.001	54.97%
Nitrate	NO^3	1254.15	8.00	0.070	8.64%	1053.85	8.68	0.114	0.00%
Organic carbon	OC	5008.99	146.00	0.070	2.47%	4599.82	240.06	0.528	0.58%
Potassium	K	74.40	3.41	0.100	0.00%	78.70	8.75	0.008	0.58%
Silicon	Si	62.02	7.53	0.100	1.23%	80.46	14.81	0.010	19.88%
Sodium	Na	77.13	51.07	0.100	56.79%	127.49	80.58	0.049	47.37%
Sulfate	SO^4	1469.51	12.00	0.050	17.28%	1403.11	12.00	0.001	0.00%
Titanium	Ti	3.64	2.08	0.070	29.63%	6.33	4.27	0.154	49.71%
Vanadium	V	2.50	1.50	0.050	51.85%	3.40	2.75	0.002	46.78%
Zinc	Zn	15.51	1.45	0.050	3.70%	14.42	2.32	0.001	8.77%

(1) The MDL values were obtained from Kim et al. (2005).

(2) Individual MDL values were given after 2003/07. Mean values were presented here.

Table 3. Source contribution estimates (in mass concentration and percentage) at Beacon Hill, estimated from the PMF and ME models with $PM_{2.5}$ data only or with $PM_{2.5}$ and VOC data combined.

Source	PM2.5 only				PM2.5 and VOC							
	PM contribution				PM contribution				VOC contribution			
	PMF		ME		PMF		ME		PMF		ME	
	ng/m^3	%	ng/m^3	%	ng/m^3	%	ng/m^3	%	ng/m^3	%	ng/m^3	%
Vegetative burning	2640	34	2256	29	2457	30	2464	31	420	11	425	10
Secondary sulfate	1704	22	1590	20	1622	20	1568	19	336	9	352	8
Nitrate rich	1253	16	1202	15	1158	14	1067	13	23	1	27	1
Diesel	772	10	505	6	784	10	745	9	504	12	519	12
Gasoline	105	1	879	11	542	7	356	4	1747	45	1787	42
Fuel	410	5	640	8	439	5	601	7	220	6	187	4
Marine	147	2	136	2	153	2	140	2	29	1	28	1
Soil	128	2	120	2	170	2	140	2	43	1	45	1
Aged sea salt	491	6	434	5	432	5	494	6	56	1	129	3
Other 1	169	2	130	2								
Other 2					424	5	340	4	352	9	588	14
Cu rich					47	1	144	2	166	5	215	5

Table 4. Source contribution estimates (in percentage) at Georgetown, estimated from the PMF and ME models with $PM_{2.5}$ data only or with $PM_{2.5}$ and VOC data combined.

Source	$PM_{2.5}$ only				$PM_{2.5}$ and VOC							
	PM contribution				PM contribution				VOC contribution			
	PMF		ME		PMF		ME		PMF		ME	
	ng/m^3	%	ng/m^3	%	ng/m^3	%	ng/m^3	%	ng/m^3	%	ng/m^3	%
Vegetative burning	5094	49	3792	37	5153	49	4919	60	2244	45	2463	40
Secondary sulfate	2645	25	1716	17	2492	24	1984	24	946	19	965	16
Diesel			289	3	478	5	592	7	611	12	788	13
Gasoline			3792	37	1978	19	497	6	1102	22	1499	24
Marine	437	4	401	4	457	4	97	1	42	1	129	2
Soil			169	2								
Other 1	946	9										
Other 2	1378	13										

Table 5. PM source contribution estimates at Portland, estimated from the PMF and ME models with speciated $PM_{2.5}$ data only.

Source	PMF		ME	
	ng/m^3	%	ng/m^3	%
Vegetative burning	3789	34	4688	44
Secondary aerosol			3522	33
Secondary sulfate	1545	14		
Nitrate rich	1970	18		
Diesel	746	7	461	4
Gasoline	1872	17		
Fuel	584	5	295	3
Marine	274	2	419	4
Soil	192	2	1654	13
other 1	168	2		

Table 6. Pearson's correlation coefficients (r) among the PM sources at Beacon Hill.

	Nitrate	Sulfate	Soil	Vegetative	Diesel	Other2	Gasoline	Age	Cu rich	Marine	Fuel
Nitrate	1.00	0.45	0.10	0.58	0.37	-0.34	0.38	-0.17	0.47	-0.04	0.09
Sulfate	0.45	1.00	0.29	0.42	0.34	-0.50	0.40	-0.13	0.26	-0.25	0.46
Soil	0.10	0.29	1.00	0.10	0.17	-0.27	0.20	0.14	0.21	-0.06	0.20
Vegetative	0.58	0.42	0.10	1.00	0.37	-0.30	0.42	-0.28	0.31	-0.11	0.11
Diesel	0.37	0.34	0.17	0.37	1.00	-0.41	0.40	-0.16	0.36	-0.10	0.35
Other2	-0.34	-0.50	-0.27	-0.30	-0.41	1.00	-0.26	-0.35	-0.29	-0.09	-0.42
Gasoline	0.38	0.40	0.20	0.42	0.40	-0.26	1.00	-0.11	0.35	-0.14	0.21
Age	-0.17	-0.13	0.14	-0.28	-0.16	-0.35	-0.11	1.00	-0.25	0.28	0.05
Cu rich	0.47	0.26	0.21	0.31	0.36	-0.29	0.35	-0.25	1.00	-0.05	0.17
Marine	-0.04	-0.25	-0.06	-0.11	-0.10	-0.09	-0.14	0.28	-0.05	1.00	-0.13
Fuel	0.09	0.46	0.20	0.11	0.35	-0.42	0.21	0.05	0.17	-0.13	1.00

Table 7. Regression coefficients obtained from the PAH stepwise regression models.

PAH	Soil	Fuel	Mobile
Pyrene	0.002061	-	-
Anthracene	-	-	-
Fluoranthene	-	-	0.000602
Fluorene	-	0.003526	0.001402
Naphthalene	-	-	-
Phenanthrene	-	0.006537	-
12dimethylnaphth	-	0.000738	-
16dimethylnaphth	-	0.000752	-
17dimethylnaphth	-	0.001766	-
23dimethylnaphth	-	0.001462	-
26dimethylnaphth	-	0.000789	0.000562
1methylphenanthr	0.002438	0.00049	-
2methylphenanthr	0.006484	-	-
Acenaphthene	-	0.00186	-
Acenaphthylene	-	-	0.000523

Table 8. Estimated PAHs concentrations (ng/m^3) from the PAH stepwise regression models.

PAH	Fuel	Mobile	Soil	Sum	Measured
12dimethylnaphth	0.324	-	-	0.324018	0.88
16dimethylnaphth	0.3303	-	-	0.330251	1.12
17dimethylnaphth	0.7758	-	-	0.775847	1.72
23dimethylnaphth	0.6423	-	-	0.642295	1.18
26dimethylnaphth	0.3468	0.74512	-	1.091907	1.57
1methylphenanthr	0.2153	-	0.4152	0.630427	1.36
2methylphenanthr	-	-	1.1043	1.104302	2.82
Acenaphthene	0.8171	-	-	0.817139	1.67
Acenaphthylene	-	0.69382	-	0.693822	1.36
Anthracene	-	-	-	-	0.95
Fluoranthene	-	0.79814	-	0.798141	1.95
Fluorene	1.5491	1.86011	-	3.409208	3.51
Naphthalene	-	-	-	-	1.21
Phenanthrene	2.8716	-	-	2.871637	10.78
Pyrene	-	-	0.351	0.351015	1.22

Table 9. Unit risks used in risk assessment.

Element	Unit risk(risk/ng/m^3)	Reference
As	4.3E-06	IRIS
Cr	2.4E-06	USEPA NATA
Pb	1.2E-08	USEPA NATA (CalEPA)
Ni	4.8E-07	USEPA NATA
1,3-Butadiene	3.0E-08	USEPA NATA (EPA NCEA)
Benzene	7.8E-09	IRIS
Carbon tetrachloride	1.5E-08	IRIS
Chloroform	2.3E-08	IRIS
Acetaldehyde	2.2E-09	IRIS
Formaldehyde	1.3E-08	IRIS
Tetrachloroethylene	5.6E-09	USEPA NATA (CalEPA)
Trichloroethylene	2.0E-09	USEPA NATA (CalEPA)

Table 10.TEF used in PAHs risk assessment.

PAH	TEF	Reference
12dimethylnaphth	Not available	
16dimethylnaphth	Not available	
17dimethylnaphth	Not available	
1methylphenanthr	Not available	
23dimethylnaphth	Not available	
26dimethylnaphth	Not available	
2methylphenanthr	Not available	
Acenaphthene	0.001	US EPA,1993
Acenaphthylene	0.001	US EPA,1993
Anthracene	0.01	US EPA,1993
Fluoranthene	0.001	US EPA,1993
Fluorene	0.001	US EPA,1993
Naphthalene	0.001	US EPA,1993
Phenanthrene	0.001	US EPA,1993
Pyrene	0.001	US EPA,1993

Table 11. Risk characterization by sources at BH, based on PMF modeling results using the combined speciated $PM_{2.5}$ and VOC data.

	Age	Fuel	Marine	Nitrate	Other 2	Cu rich	Soil	Sulfate	Vegetative	Diesel	Gasoline
As	3.06E-07	1.85E-07	2.17E-08	4.34E-08	8.41E-07	1.50E-08	2.17E-08	8.51E-08	3.70E-06	2.95E-07	7.15E-08
Cr	3.63E-07	5.44E-07	9.69E-08	1.17E-09	1.75E-06	3.58E-09	3.81E-07	1.25E-09	3.00E-10	2.08E-06	2.20E-07
Ni	3.85E-08	5.82E-07	1.18E-08	1.69E-08	7.85E-10	1.20E-10	2.96E-09	8.50E-08	8.70E-11	3.06E-07	5.27E-08
Pb	1.01E-08	3.94E-09	2.05E-11	9.56E-10	1.16E-08	7.74E-10	2.72E-11	1.86E-09	1.73E-08	1.18E-08	3.91E-09
Acetaldehyde	1.66E-07	4.72E-07	9.14E-09	3.29E-08	5.93E-07	2.58E-07	1.60E-10	3.33E-10	1.20E-07	2.96E-10	1.34E-06
Benzene	7.94E-10	5.82E-10	1.17E-07	8.63E-07	1.56E-06	4.28E-07	1.88E-07	6.17E-08	1.87E-06	1.77E-06	1.90E-06
Butadiene	3.32E-07	7.99E-08	2.05E-09	3.39E-08	1.55E-06	9.08E-09	2.60E-09	1.44E-07	1.22E-06	9.28E-07	1.31E-07
Carbon tetrachloride	1.46E-06	3.00E-07	2.02E-07	9.86E-09	4.64E-06	8.08E-07	4.56E-09	1.21E-06	5.69E-07	3.92E-07	1.70E-09
Chloroform	5.13E-07	1.86E-07	1.78E-08	3.75E-08	2.57E-06	9.14E-08	2.88E-07	8.35E-07	1.41E-07	2.61E-10	7.19E-07
Formaldehyde	1.43E-06	1.03E-06	1.36E-08	4.10E-09	1.47E-06	2.93E-09	3.42E-07	1.90E-06	1.36E-09	9.51E-07	1.18E-05
Tetrachloroethylene	5.88E-08	4.24E-10	6.49E-09	6.78E-10	2.44E-07	2.79E-07	8.59E-09	8.08E-08	1.05E-07	1.24E-07	8.48E-08
Trichloroethylene	7.25E-08	1.80E-08	4.04E-09	6.15E-11	1.89E-07	5.48E-11	6.45E-09	3.84E-08	2.79E-08	4.62E-08	1.62E-08
Acenaphthene	-	8.99E-10	-	-	-	-	-	-	-	-	
Acenaphthylene	-	-	-	-	-	-	-	-	-	7.63E-10	
Fluoranthene	-	-	-	-	-	-	-	-	-	8.78E-10	
Fluorene	-	1.70E-09	-	-	-	-	-	-	-	2.05E-09	
Naphthalene	-	-	-	-	-	-	-	-	-	-	
Phenanthrene	-	3.16E-09	-	-	-	-	-	-	-	-	
Pyrene	-	-	-	-	-	-	3.86E-10	-	-	-	
Sum of PM	7.18E-07	1.31E-06	1.30E-07	6.24E-08	2.60E-06	1.95E-08	4.06E-07	1.73E-07	3.72E-06	2.69E-06	3.48E-07
Sum of VOCs	4.03E-06	2.09E-06	3.72E-07	9.82E-07	1.28E-05	1.88E-06	8.40E-07	4.27E-06	4.05E-06	4.21E-06	1.60E-05
Sum of PAHs	-	5.76E-09	-	-	-	-	3.86E-10	-	-	3.69E-09	
Sum of All	4.75E-06	3.41E-06	5.03E-07	1.04E-06	1.54E-05	1.90E-06	1.25E-06	4.44E-06	7.77E-06	2.32E-05	

Figure 1. Scatter plot of organic carbon vs. total $PM_{2.5}$ mass concentrations at BH. The intercept indicates the average blank value.

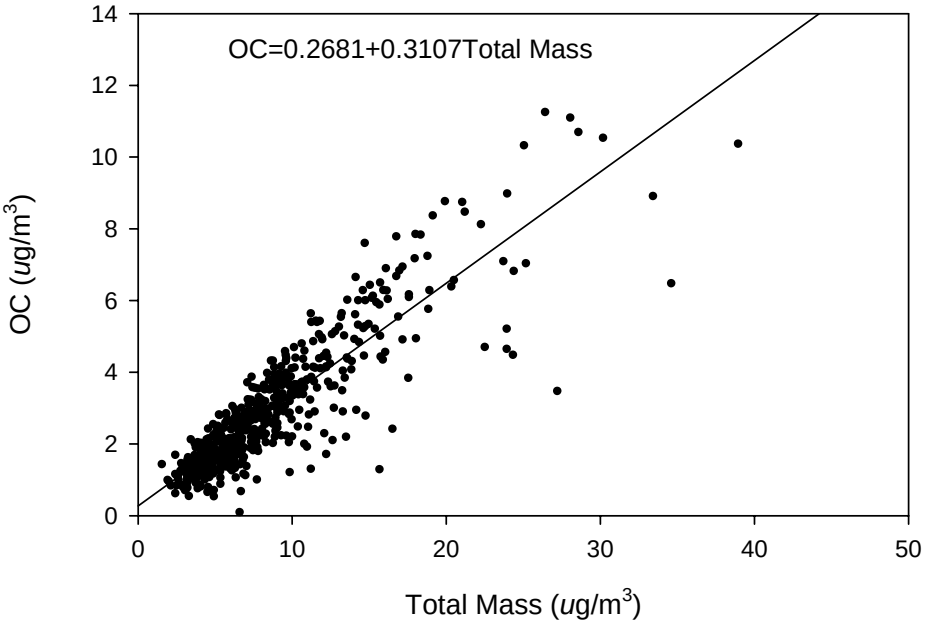

Figure 2. Scatter plot of organic carbon vs. total $PM_{2.5}$ mass concentrations at RL. The intercept indicates the average blank value.

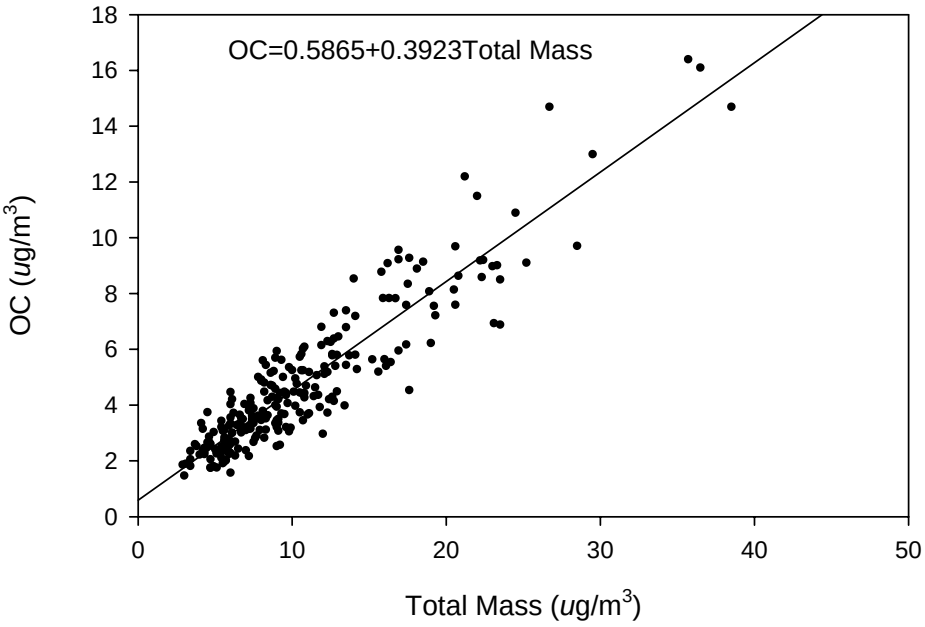

Figure 3. Source features from the PMF model using only speciated $PM_{2.5}$ data at the Beacon Hill site. (N=268 from 2000-2004)

Vegetative burning

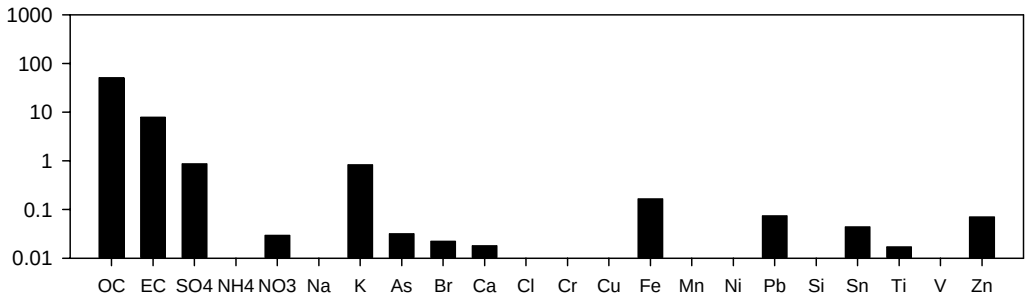

Secondary sulfate

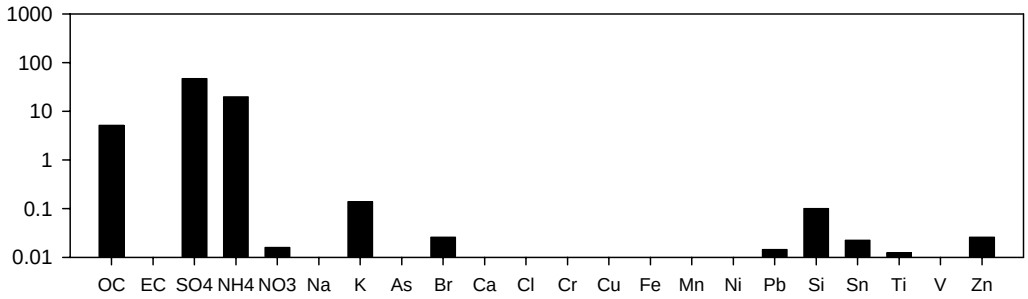

Nitrate rich

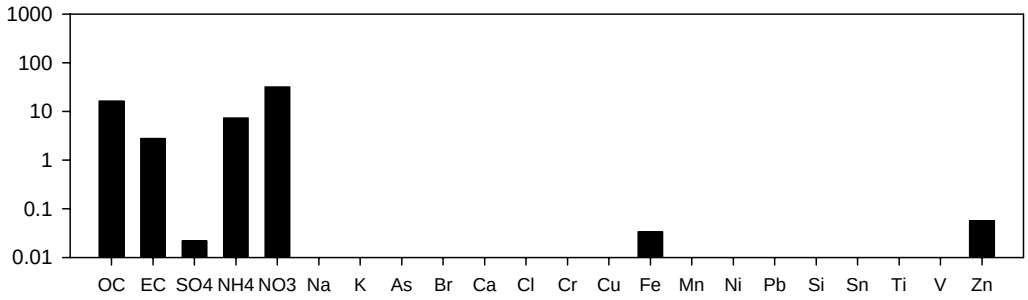

Diesel

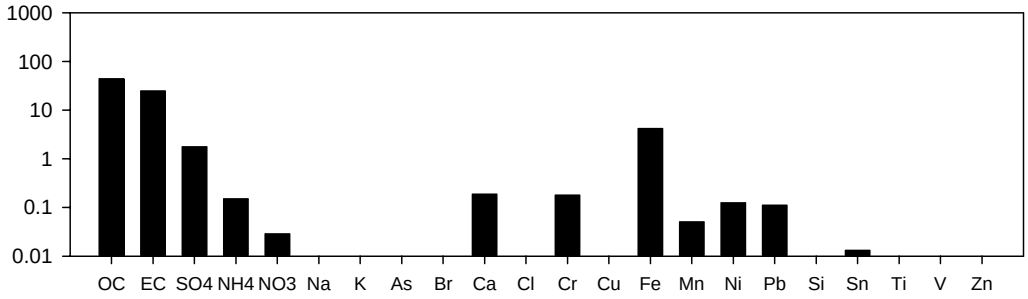

Gasoline

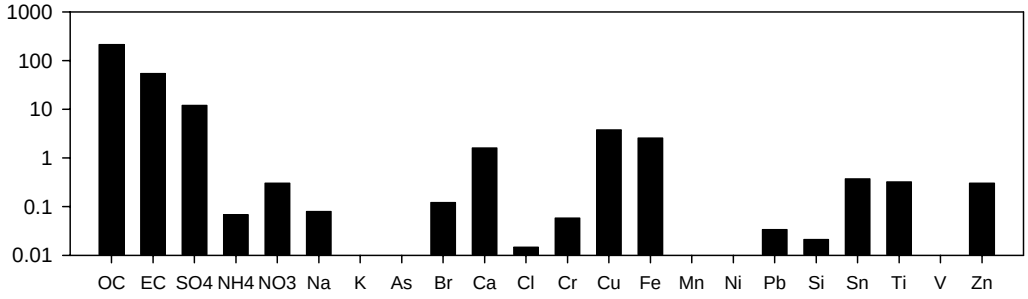

Fuel

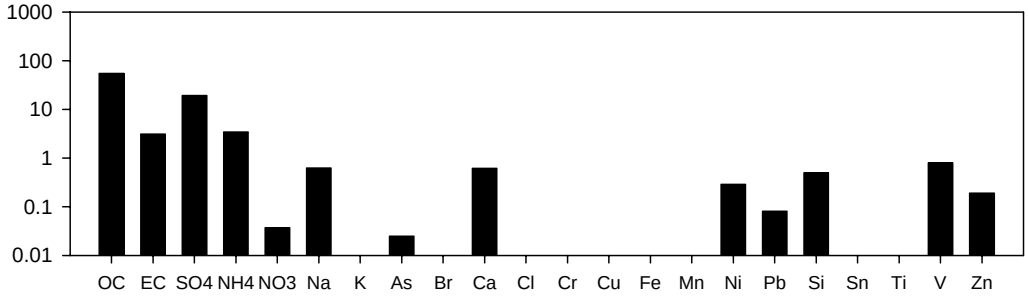

Marine

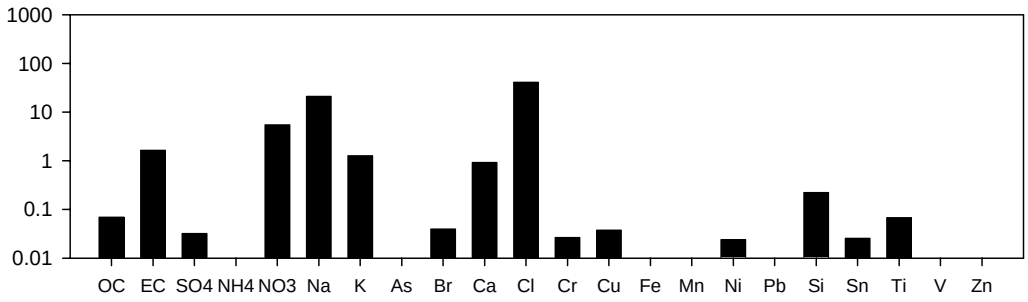

Soil

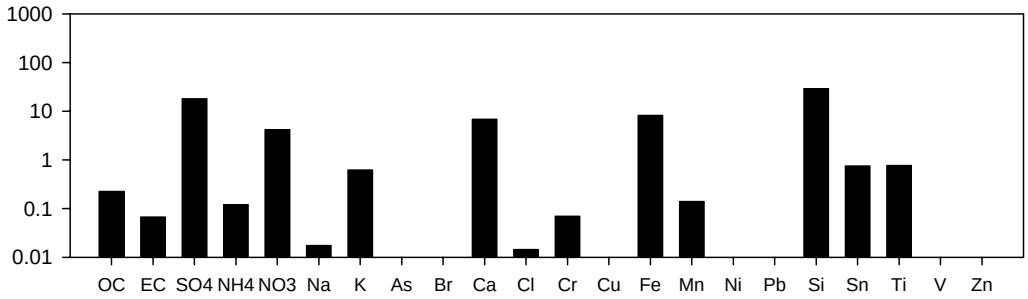

Aged sea salt

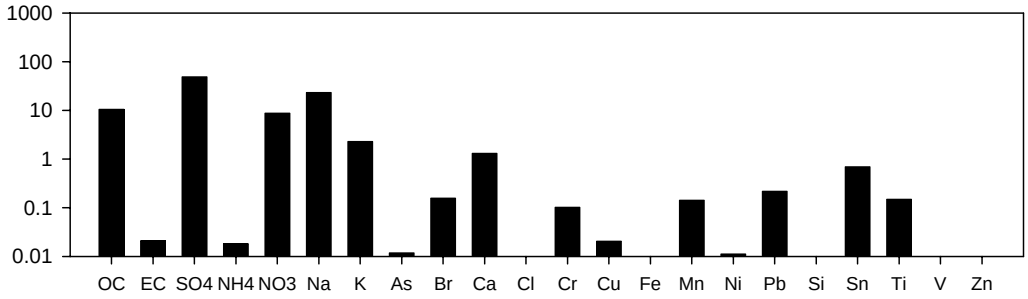

Other1

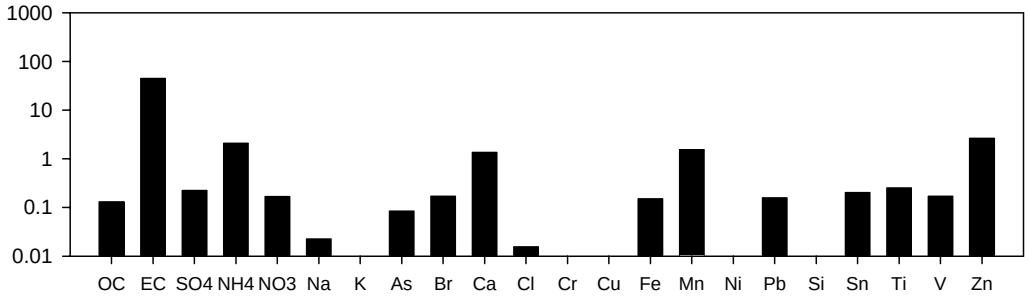
1000
100
10
1
0.1
0.01
OC EC SO4 NH4 NO3 Na K As Br Ca Cl Cr Cu Fe Mn Ni Pb Si Sn Ti V Zn

Figure 4. Source contribution estimates (SCE) between heating/non-heating seasons and weekend/weekday form PMF model

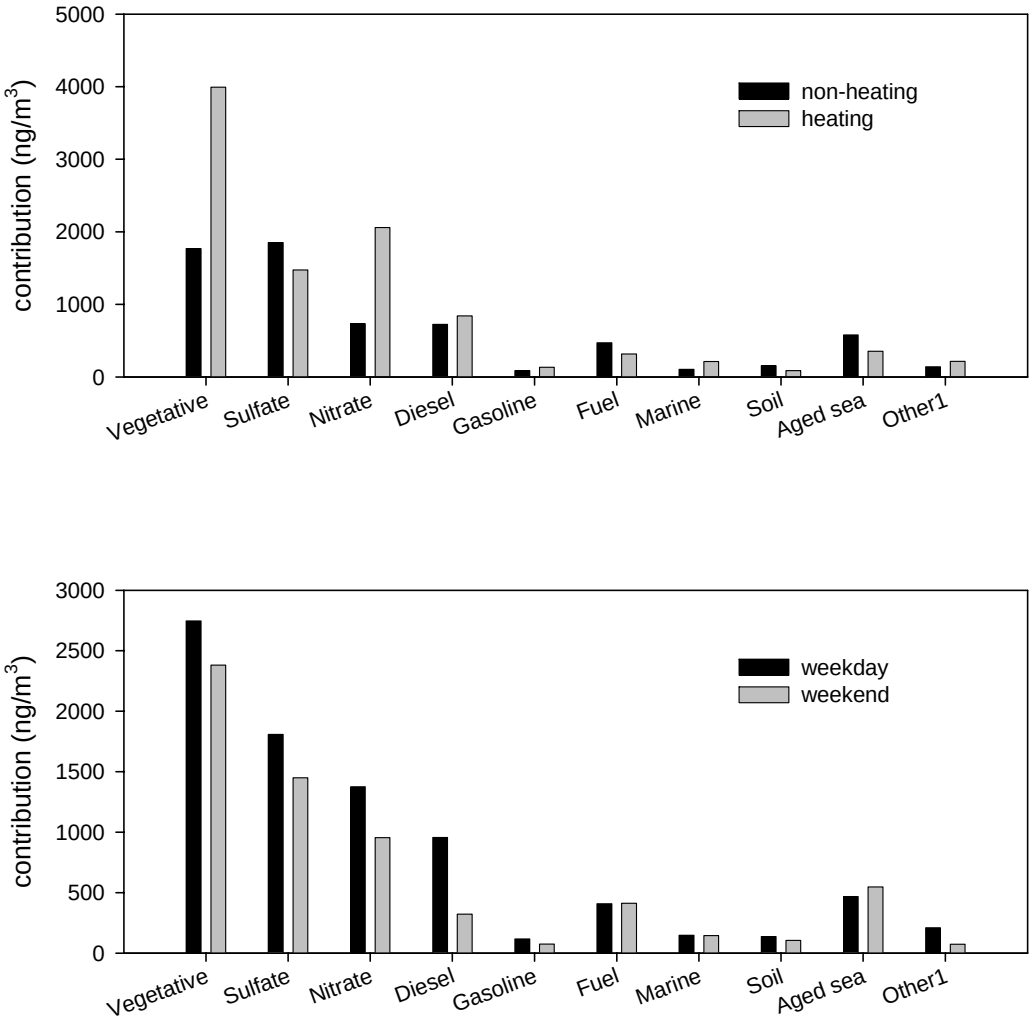

Figure 5. Source features from the ME model using only speciated $PM_{2.5}$ data at the Beacon Hill site. (N=268 from 2000-2004)

Vegetative burning

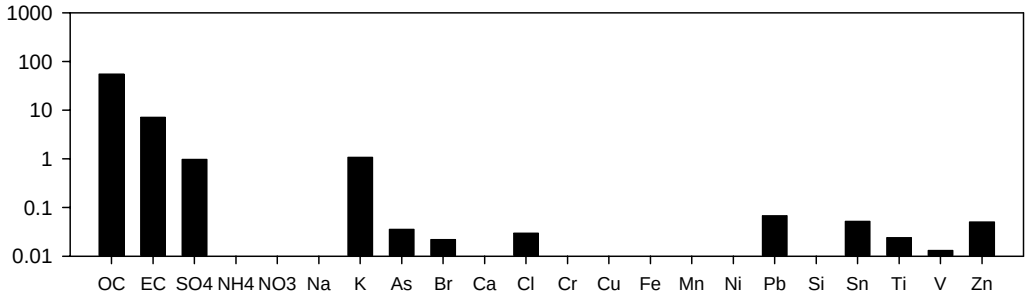

Secondary sulfate

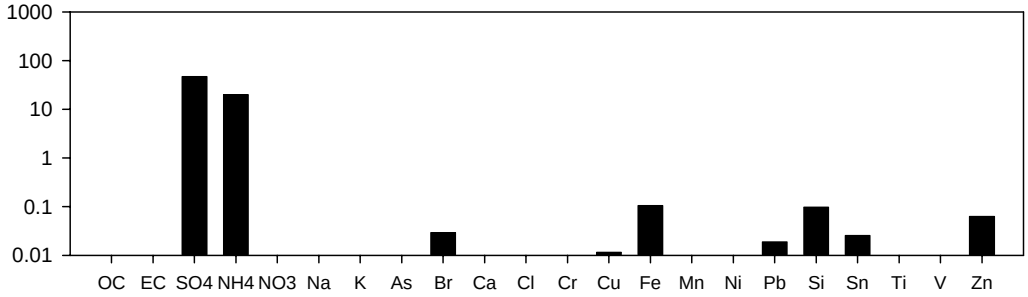

Nitrate rich

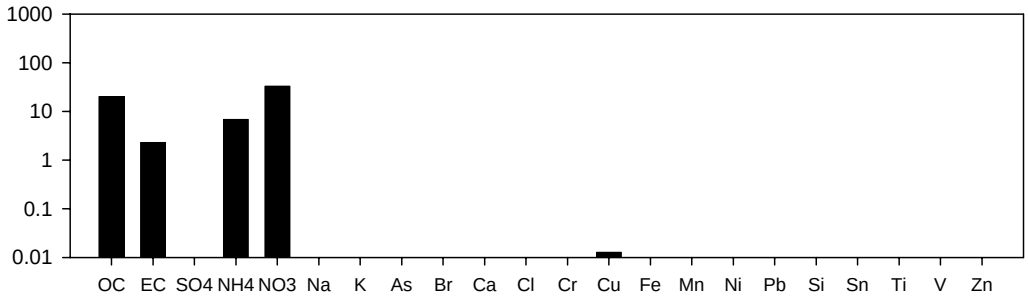

Diesel

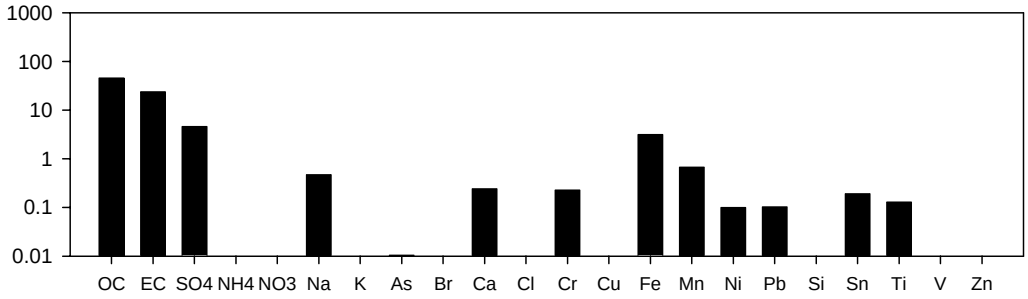

Gasoline

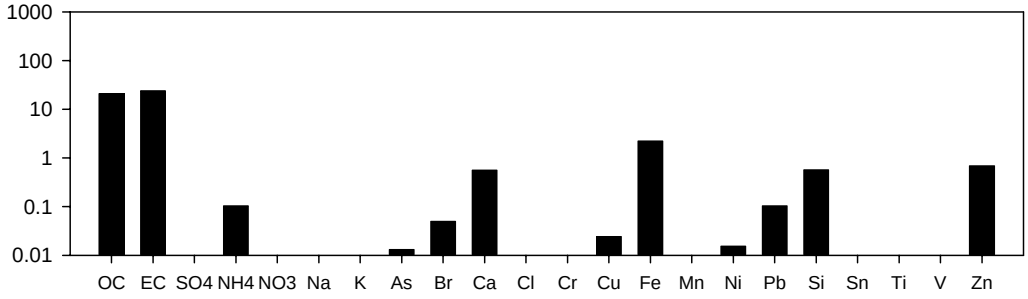

Fuel

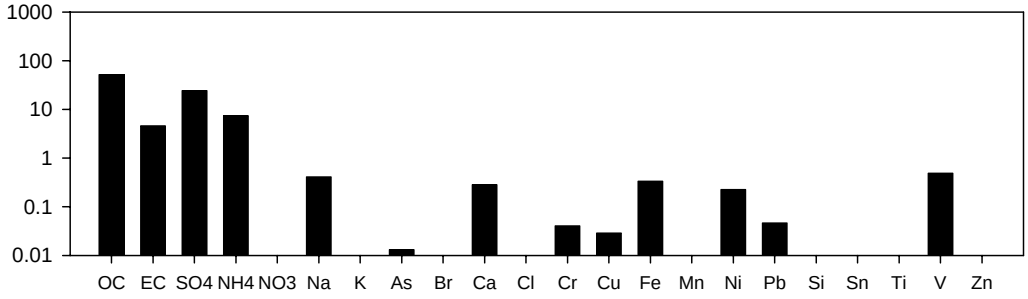

Marine

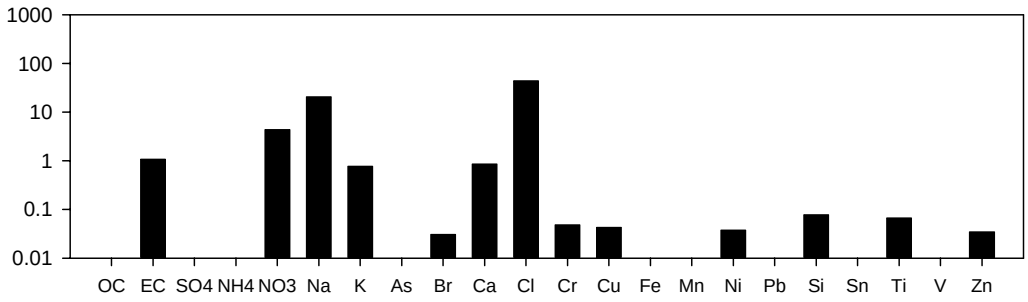

Soil

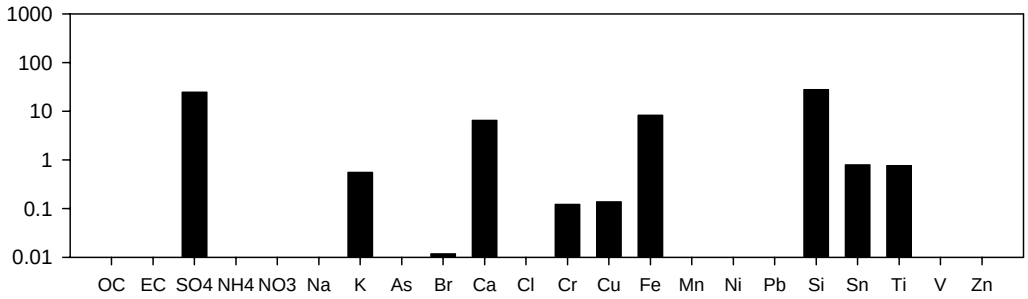

Aged sea salt

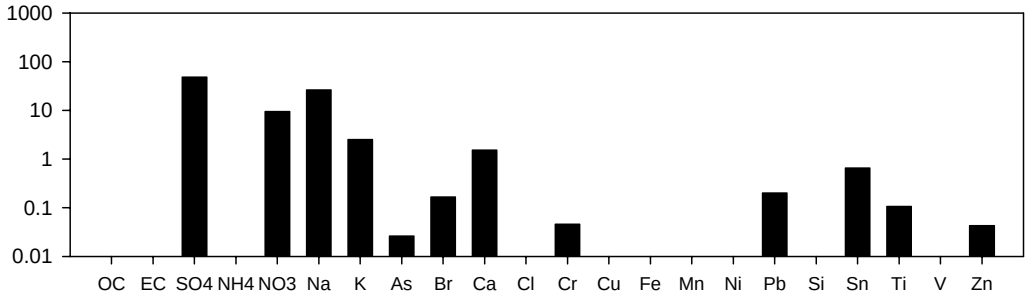

Other 1

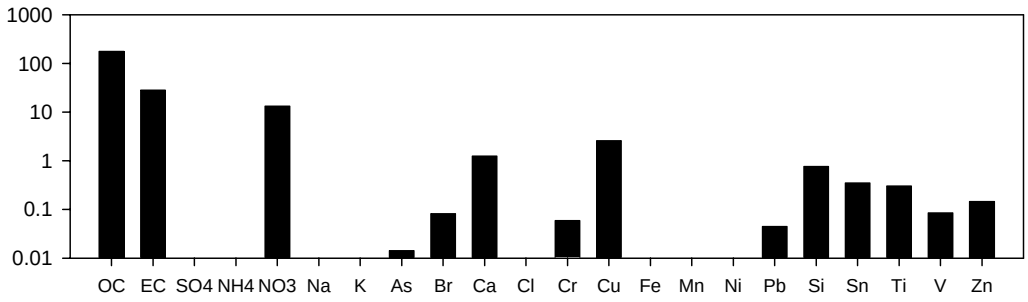
1000
100
10
1
0.1
0.01
OC
EC
SO4
NH4
NO3
Na
K
As
Br
Ca
Cl
Cr
Cu
Fe
Mn
Ni
Pb
Si
Sn
Ti
V
Zn

Figure 6. Source contribution estimates (SCE) between heating/non-heating seasons and weekend/weekday form ME model

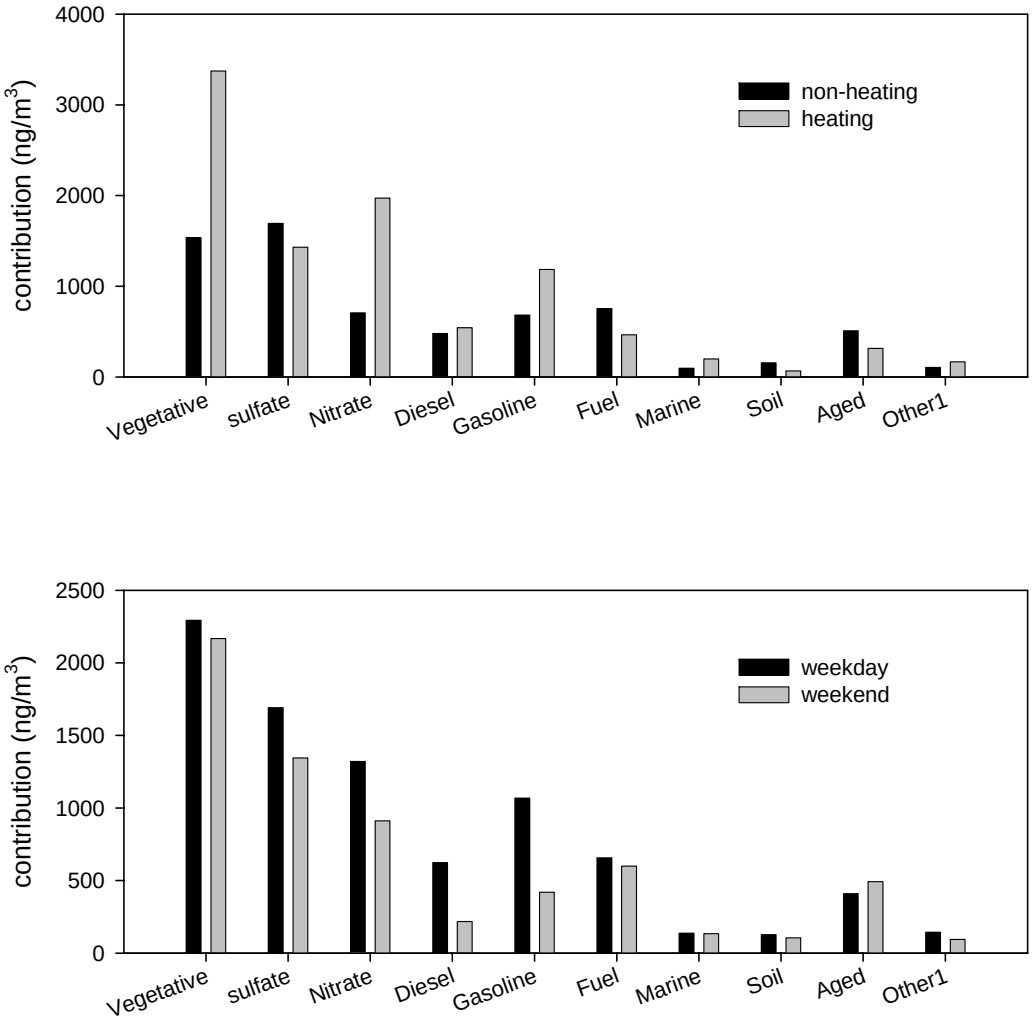

Figure 7. Source features from the PMF model using 23 $PM_{2.5}$ species and 8 VOCs at the Beacon Hill site. (N=262 from 2000-2004)

Vegetative burning

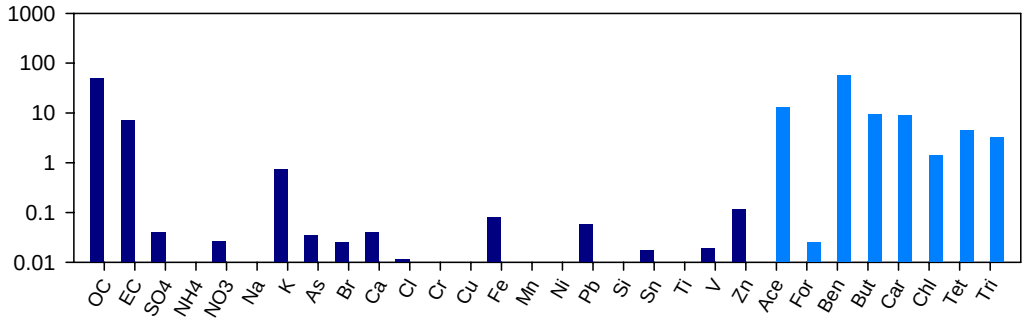

Secondary sulfate

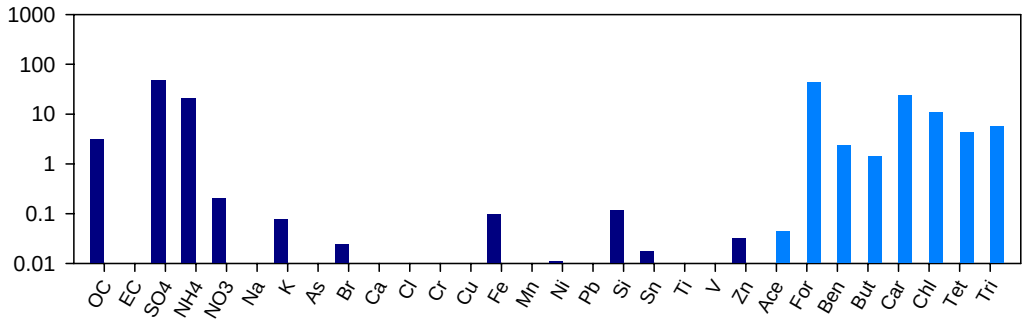

Nitrate rich

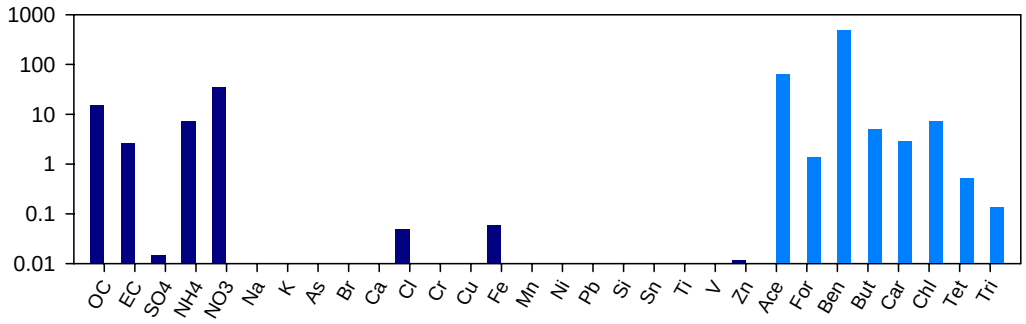

Diesel

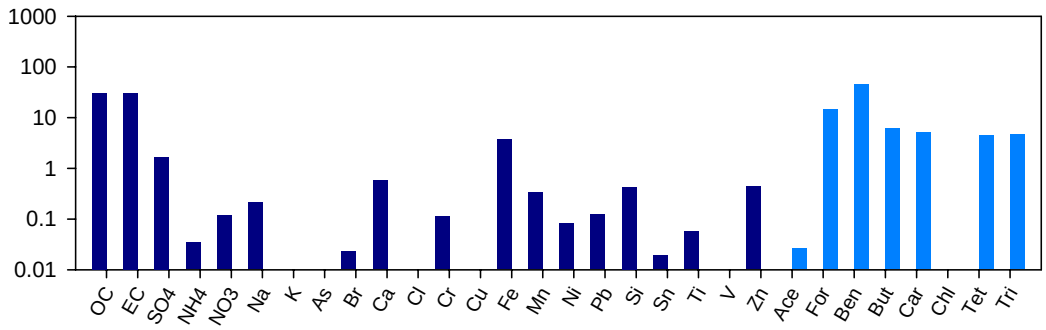

Gasoline

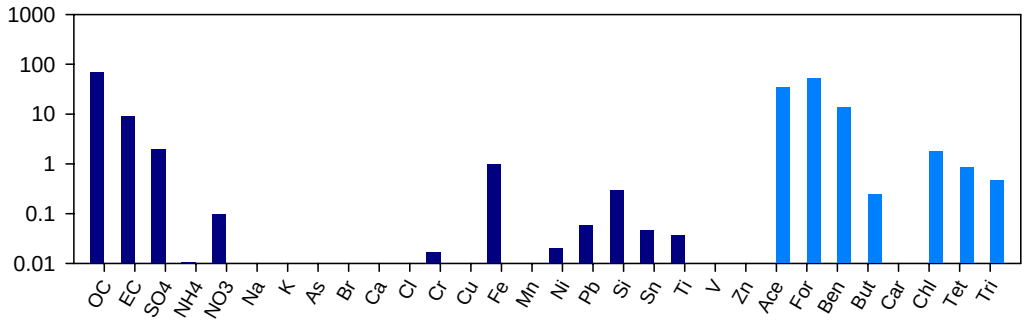

Fuel

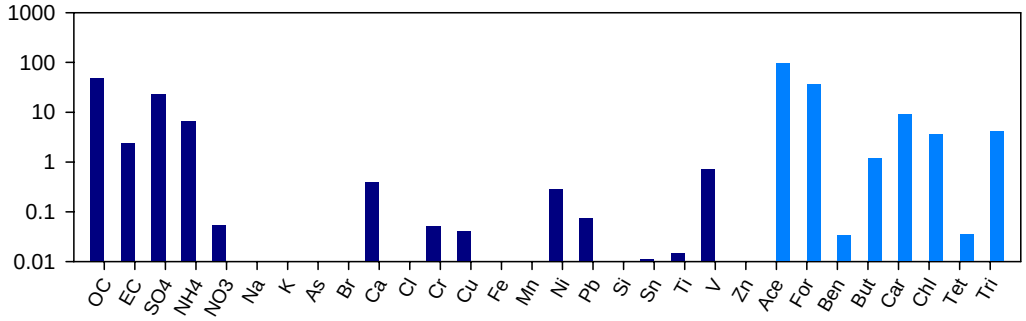

Marine

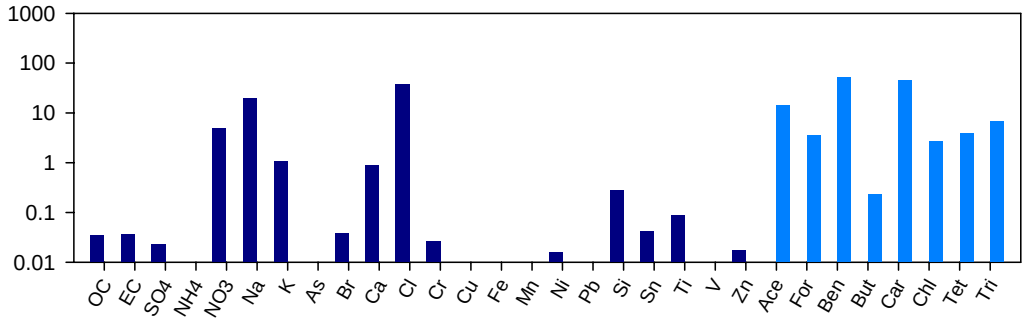

Soil

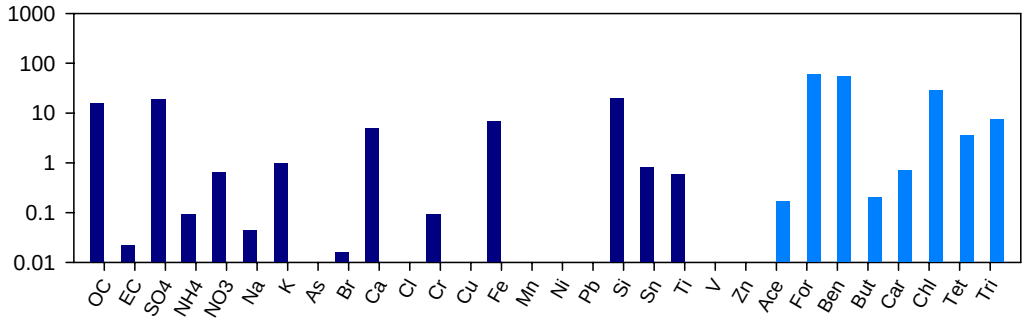

Aged sea salt

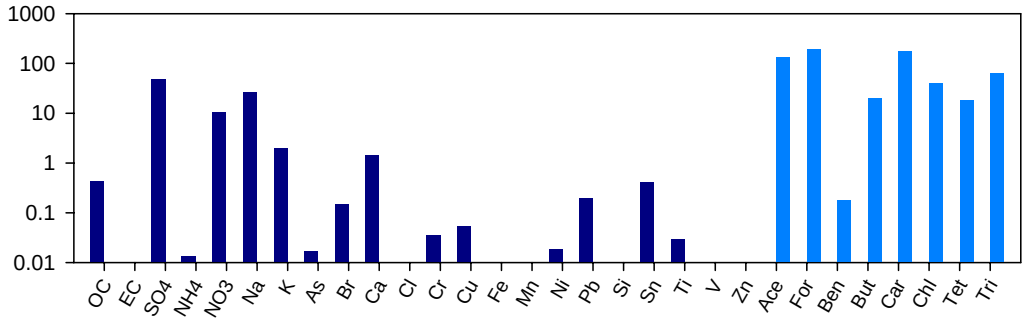

Other 2

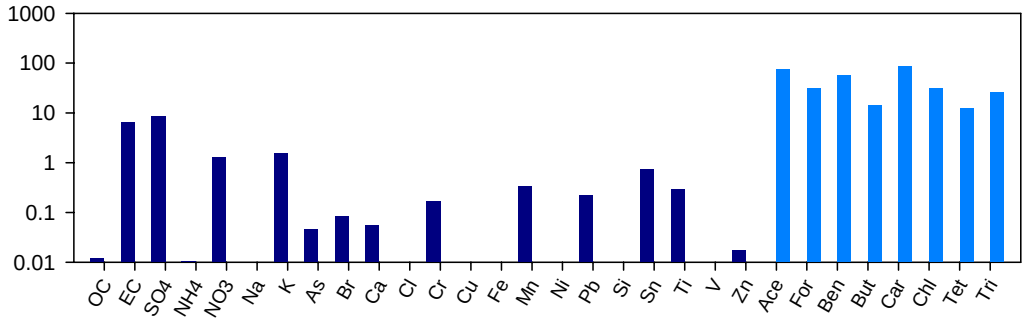

Cu rich

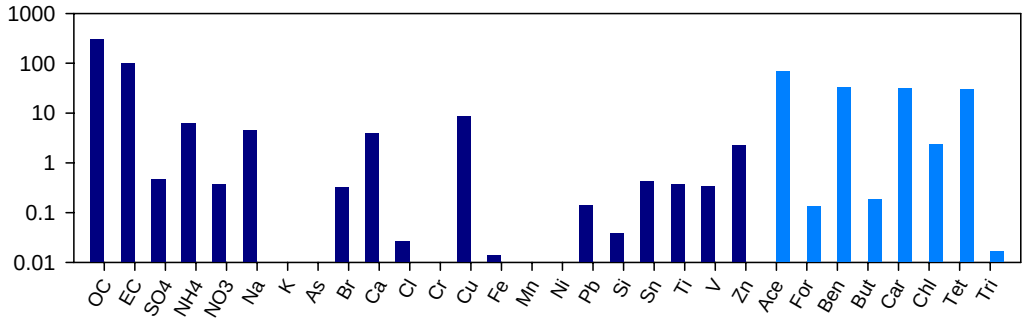

Figure 8. Source contribution estimates (SCE) between heating/non-heating seasons and weekend/weekday form PMF model.

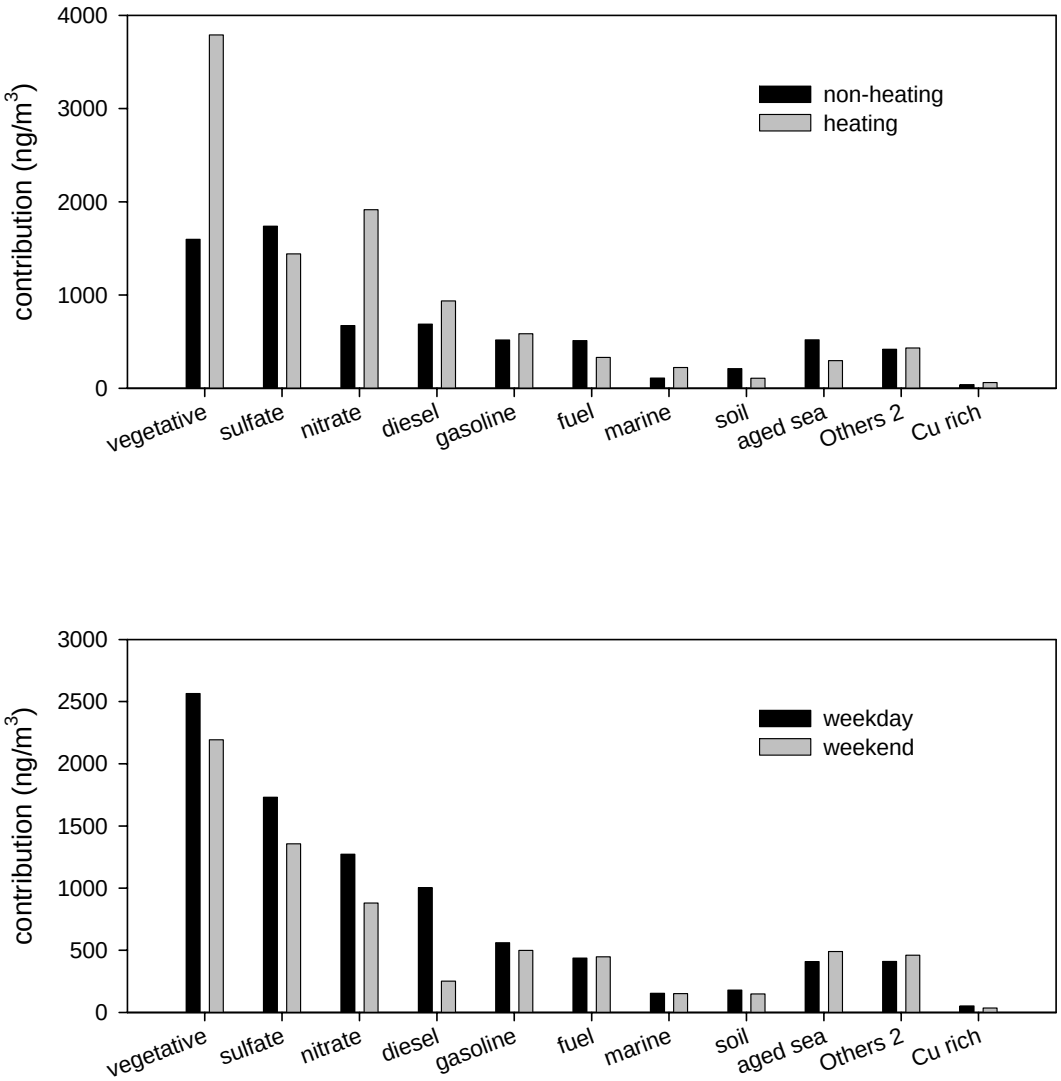

Figure 9. Source features from the ME model using 23 $PM_{2.5}$ species and 8 VOCs at the Beacon Hill site. (N=262 from 2000-2004)

Vegetative burning

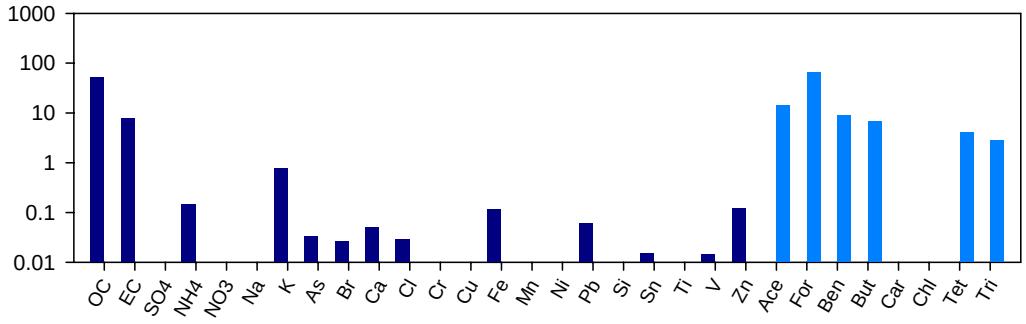

Secondary sulfate

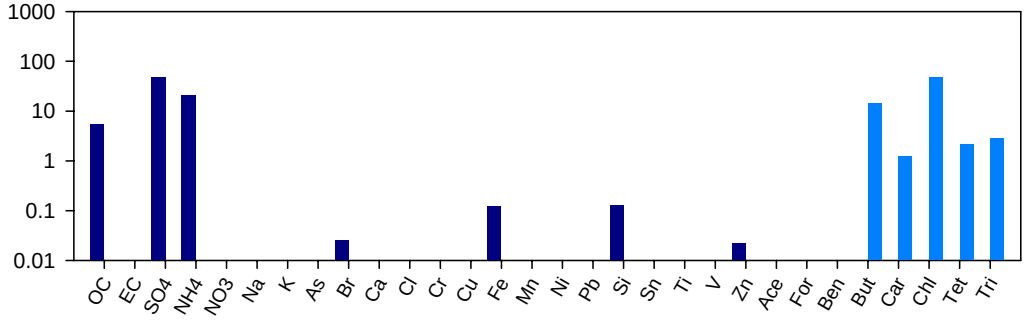

Nitrate rich

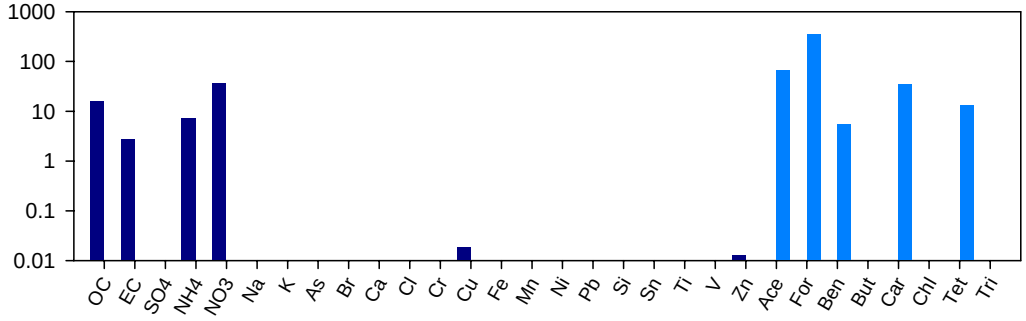

Diesel

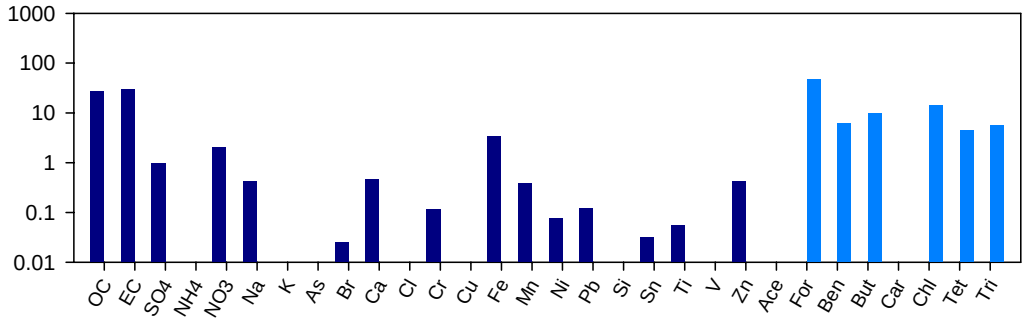

Gasoline

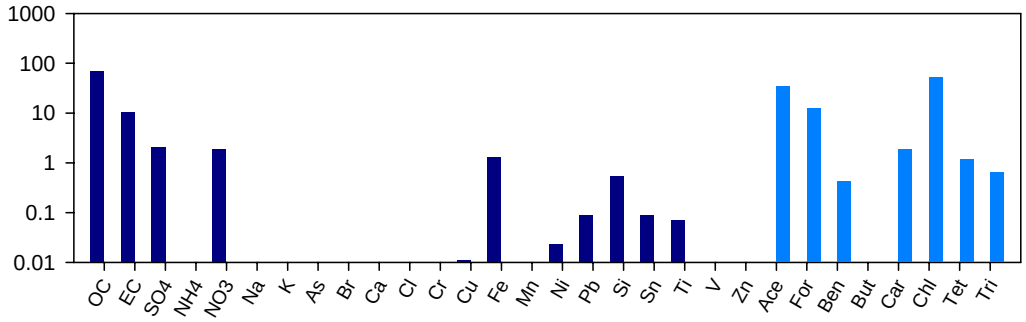

Fuel

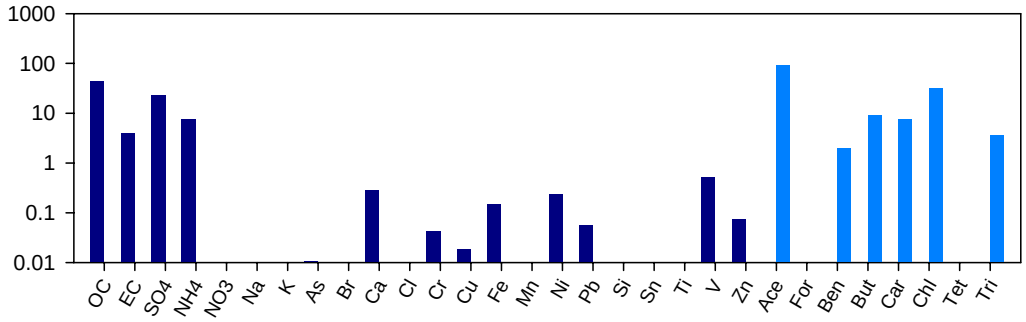

Marine

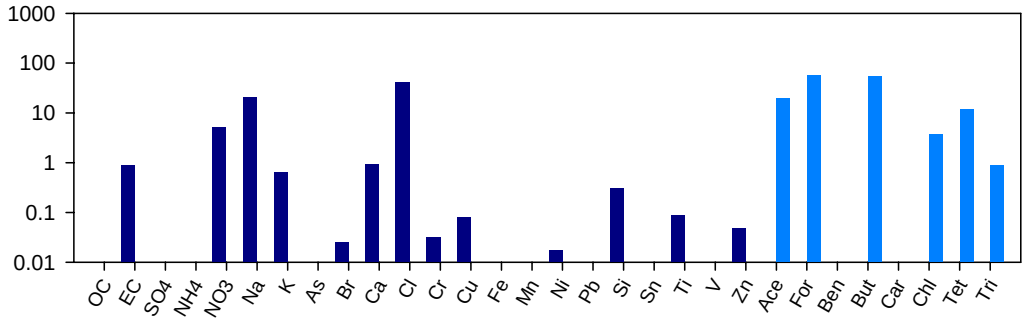

Soil

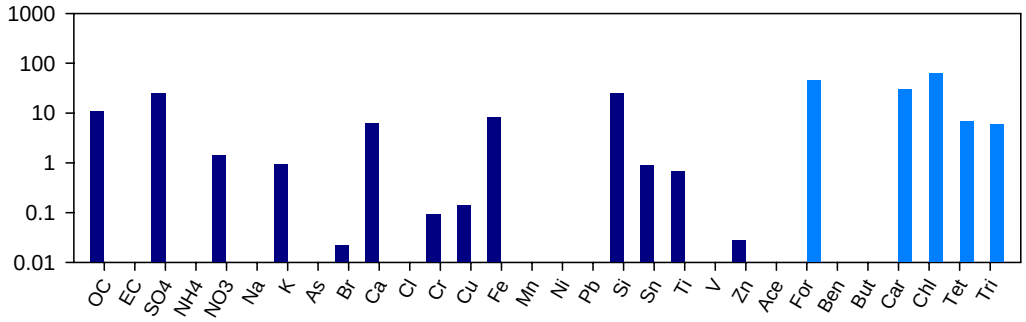

Aged sea salt

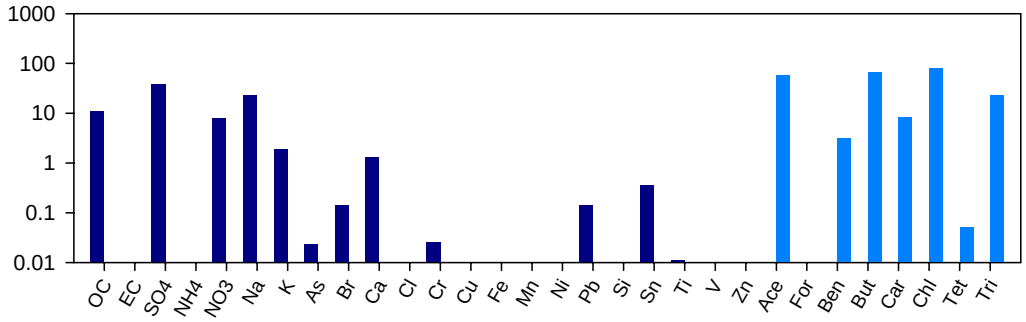

Other 2

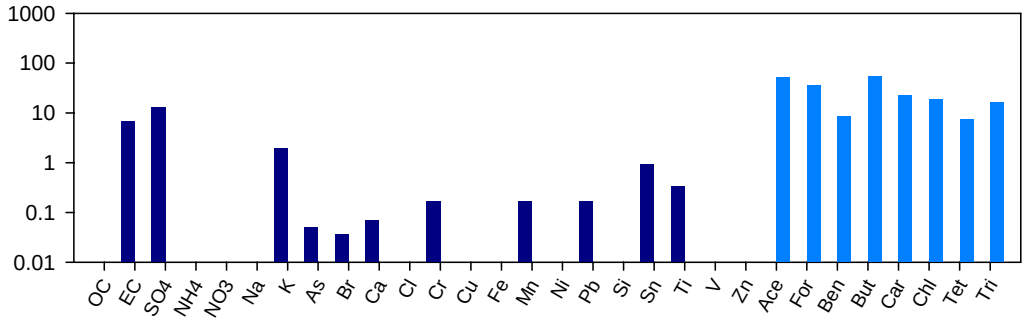

Cu rich

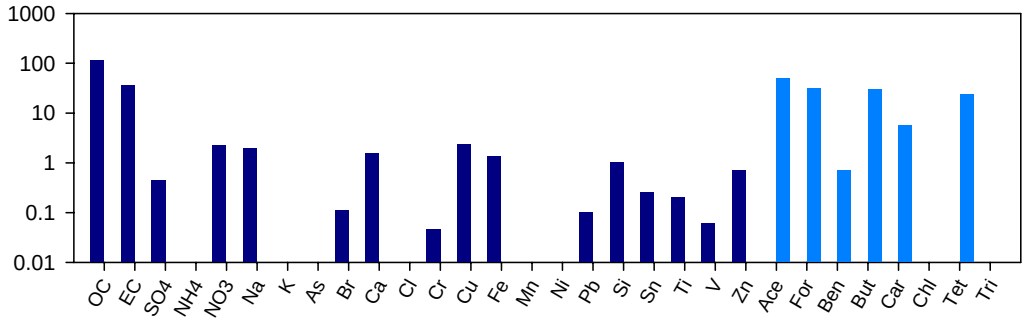

Figure 10. Source contribution estimates (SCE) between heating/non-heating seasons and weekend/weekday form ME model

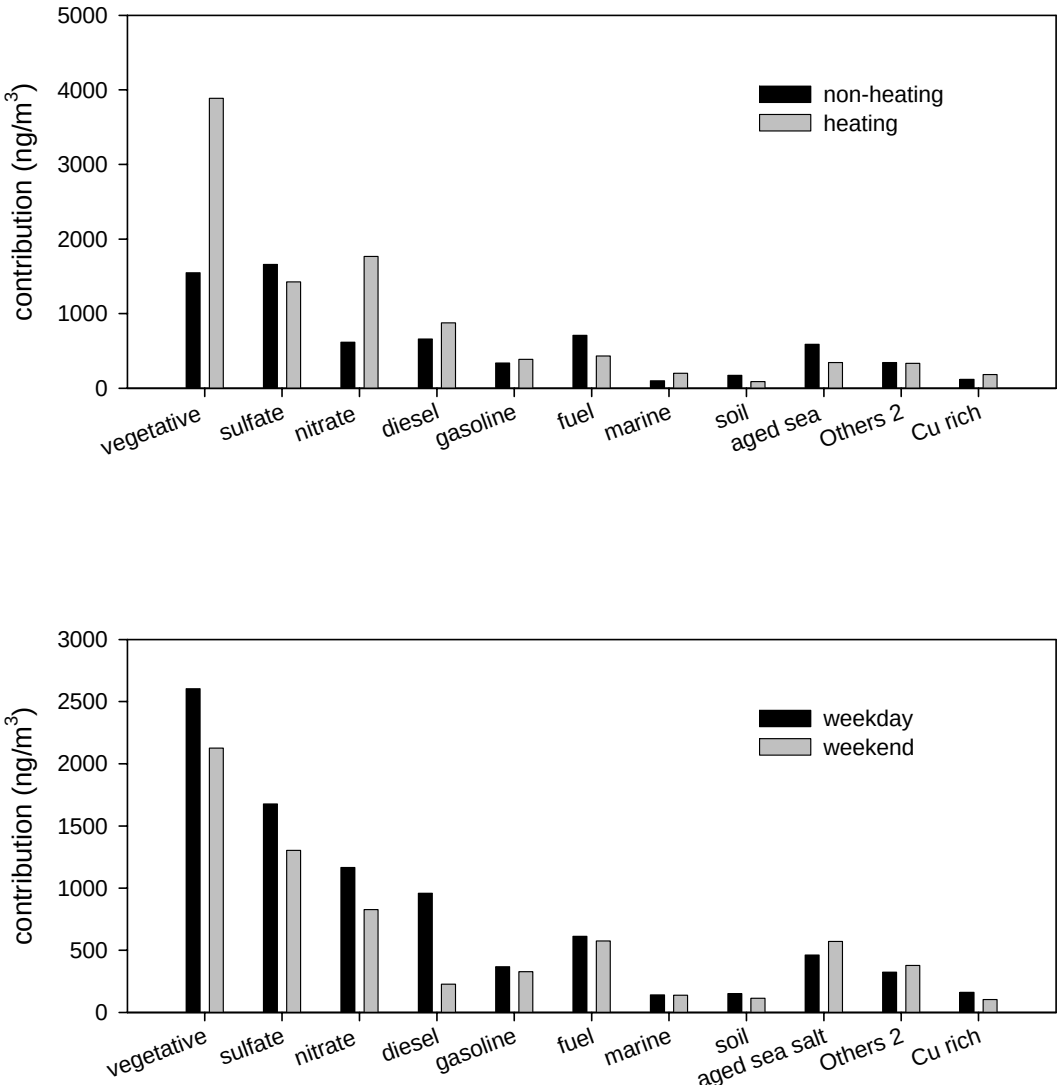

Figure 11. Source features from the PMF model using 24 $PM_{2.5}$ species only at the Georgetown site. (N=124 from 2000-2003.3)

Other 1

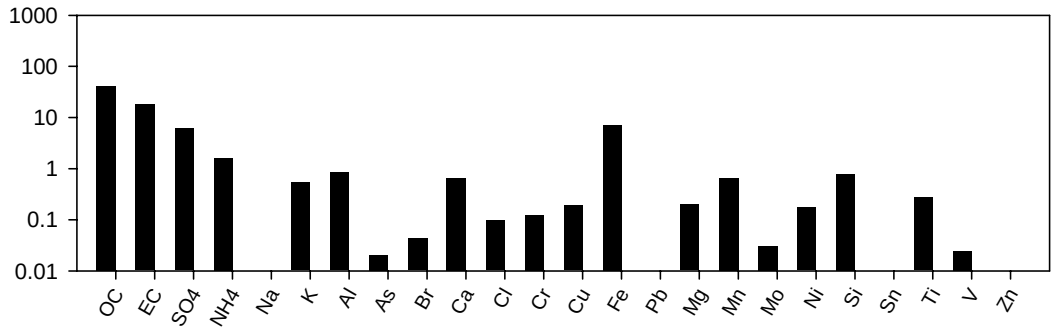

Vegetative burning

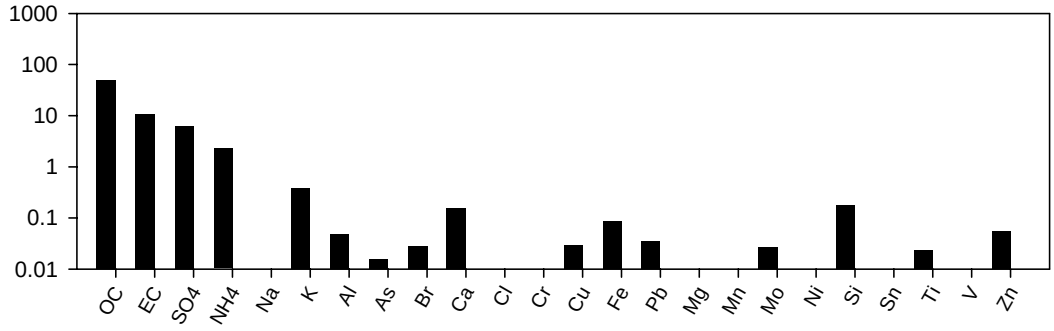

Secondary sulfate

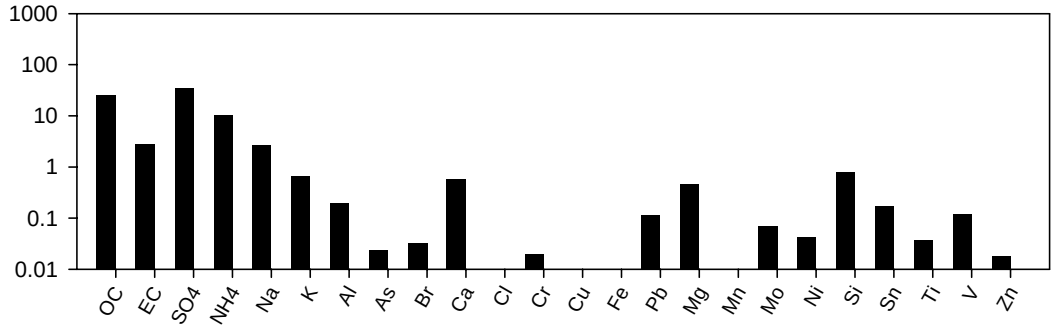

Other 2

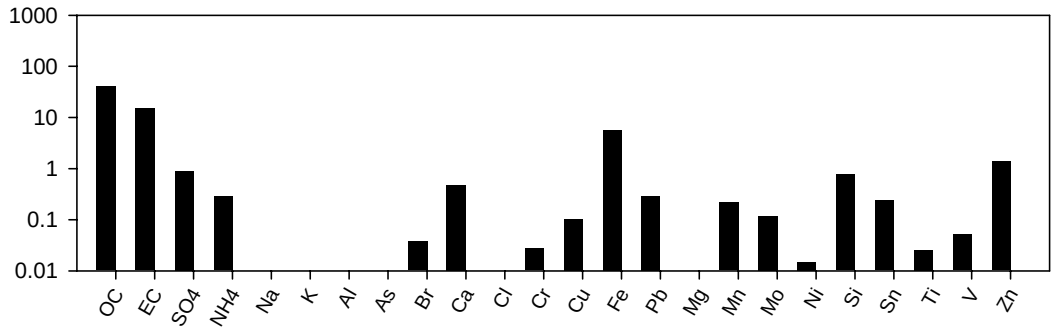

Marine

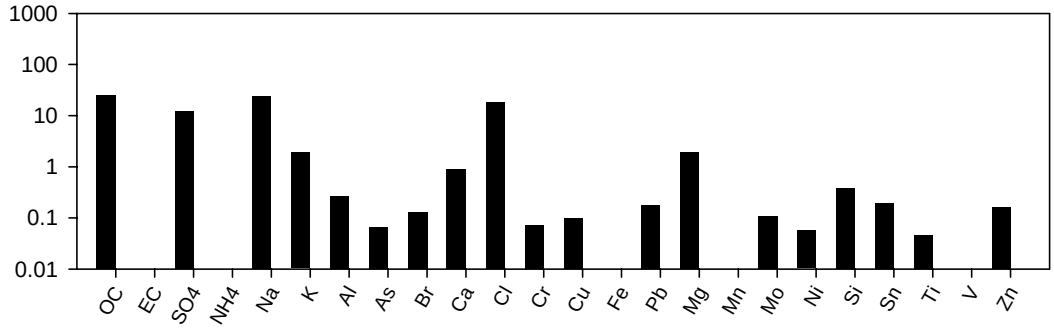

Figure 12. Source features from the ME model using 24 $PM_{2.5}$ species only at the Georgetown site. (N=123 from 2000-2003.3)

Diesel

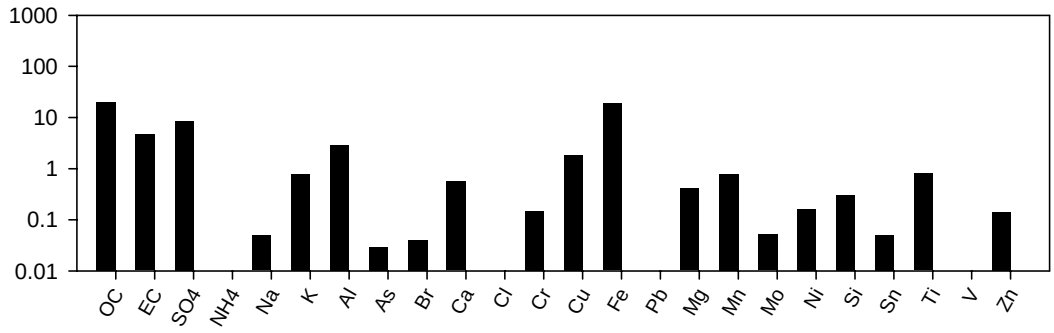

Secondary sulfate

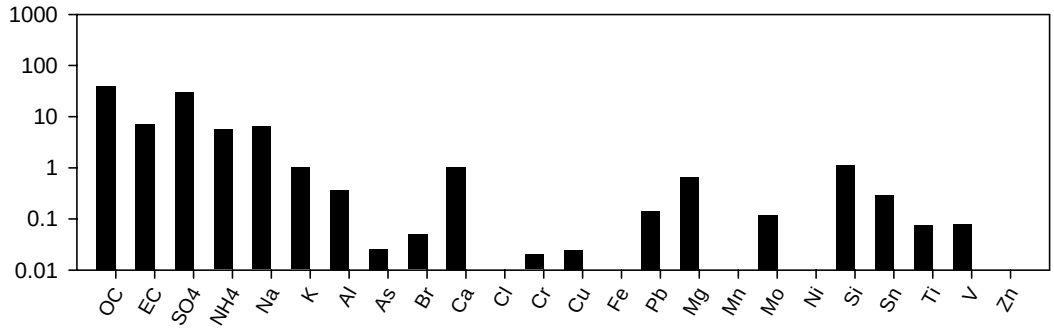

Vegetative burning

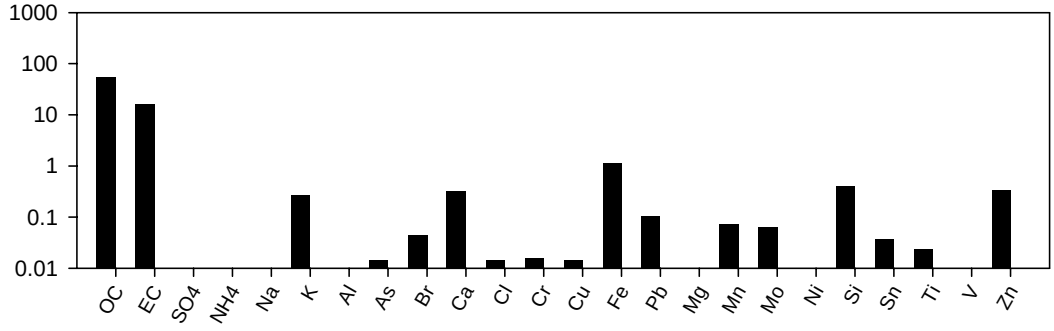

Marine

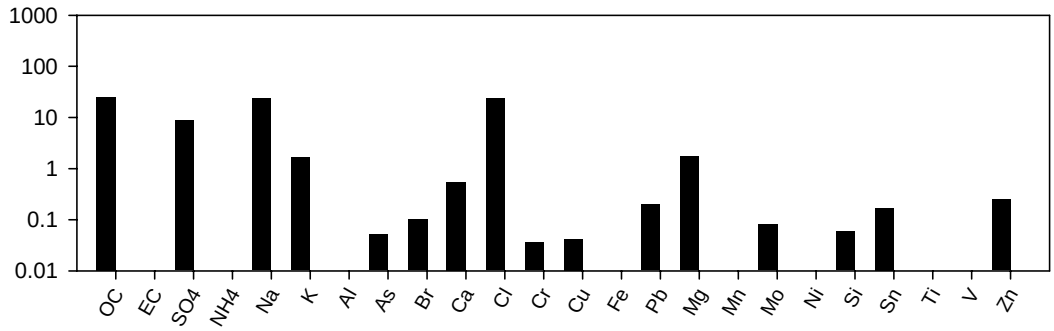

Gasoline

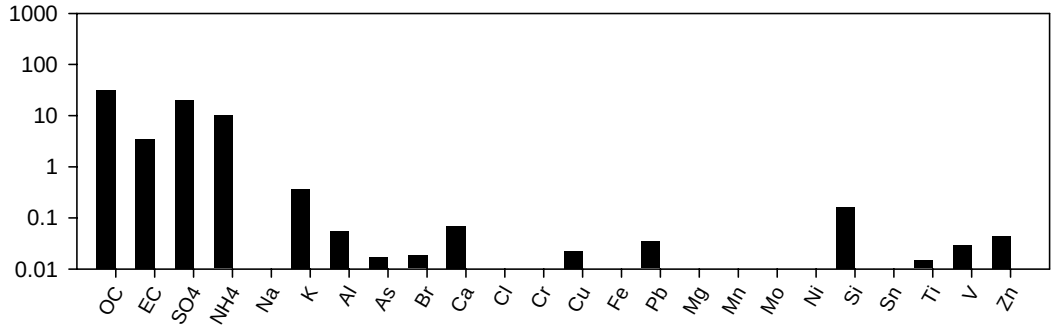

Soil

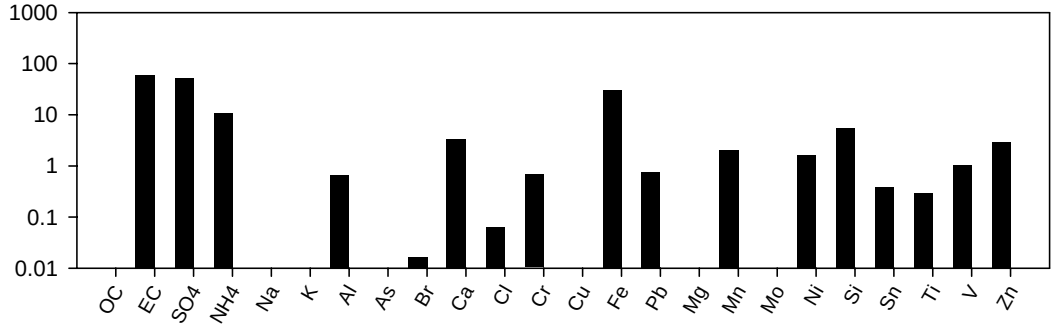

Figure 13. Source features from the PMF model using 24 $PM_{2.5}$ species and 8 VOCs at the Georgetown site. (N=123 from 2000-2003.3)

Marine

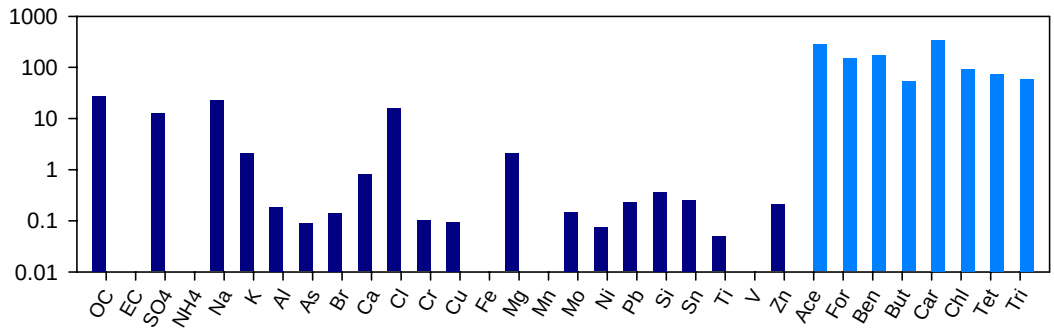

Vegetative burning

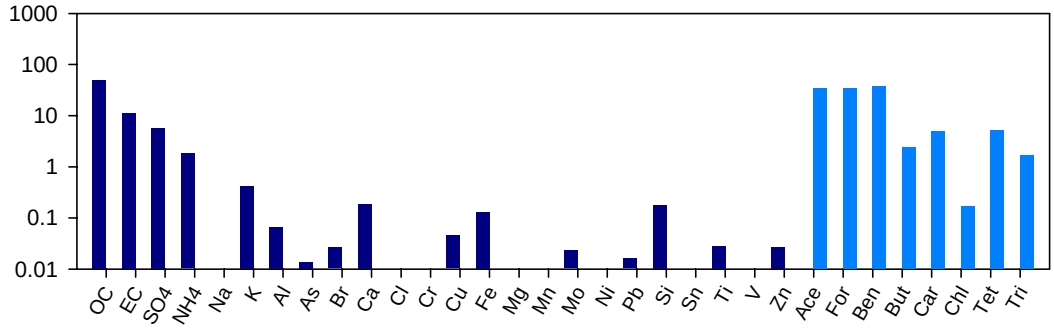

Gasoline

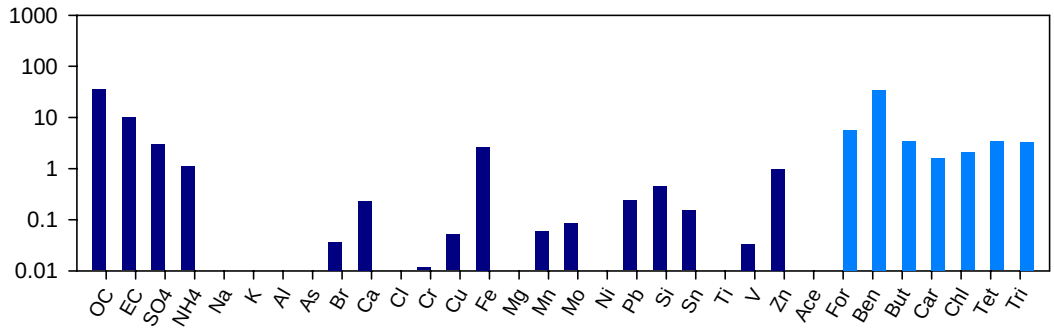

Secondary sulfate

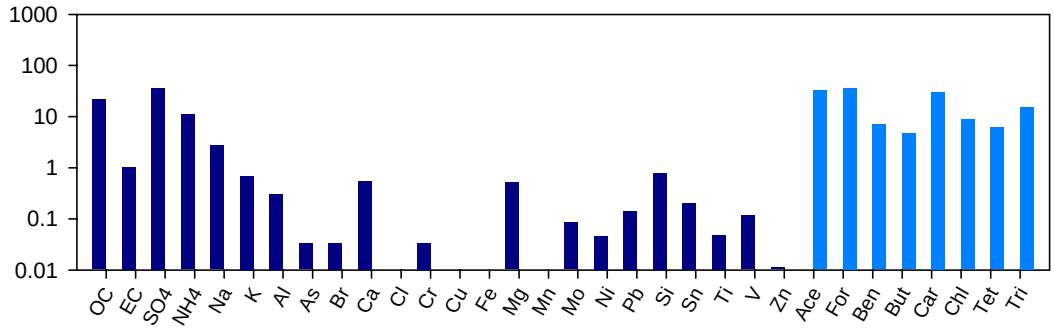

Diesel

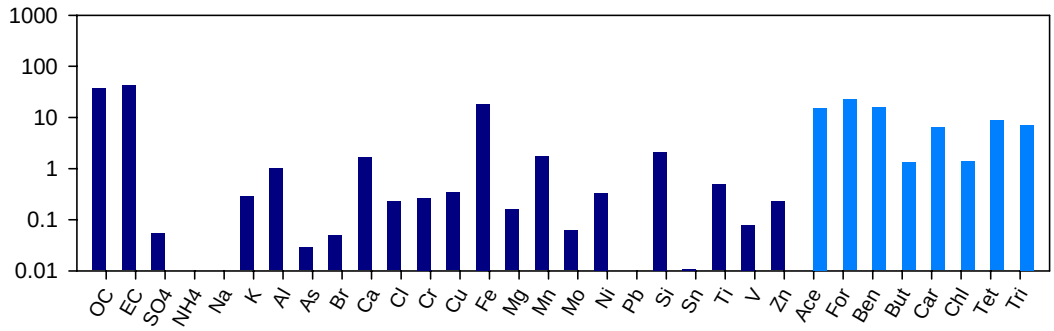
1000
100
10
1
0.1
0.01
OC
EC
SO4
NH4
Na
K
Al
As
Br
Ca
Cl
Cr
Cu
Fe
Mg
Mn
Mo
Ni
Pb
Si
Sn
Ti
V
Zn
Ace
For
Ben
But
Car
Chl
Tet
Tri

Figure 14. Source features from the ME model using 24 $PM_{2.5}$ species and 8 VOCs at the Georgetown site. (N=123 from 2000-2003.3)

Soil

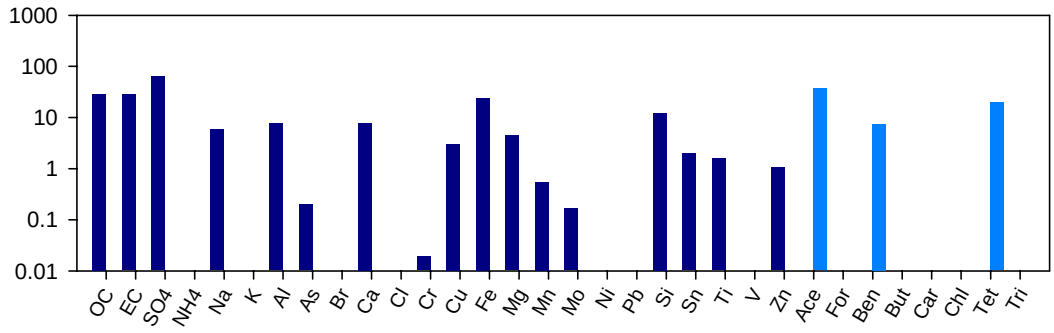

Gasoline

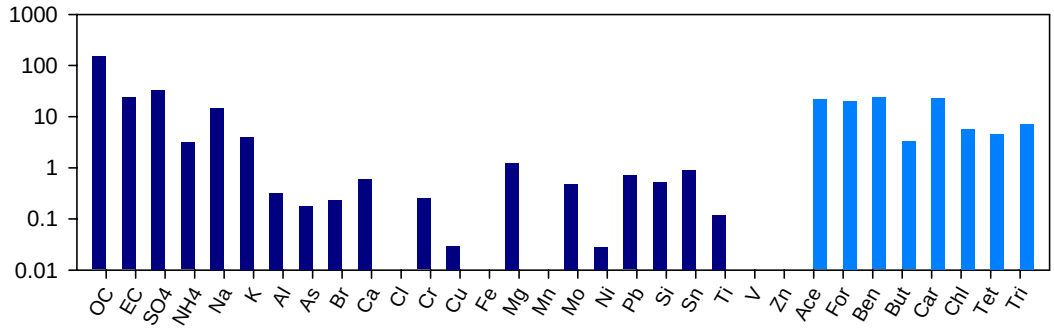

Vegetative

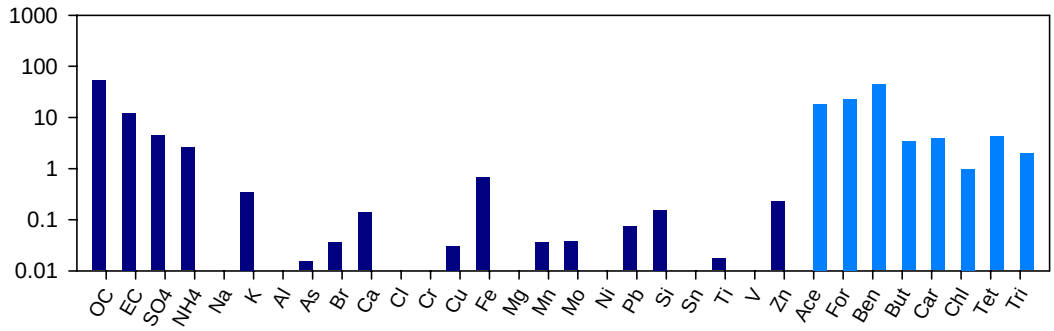

Marine

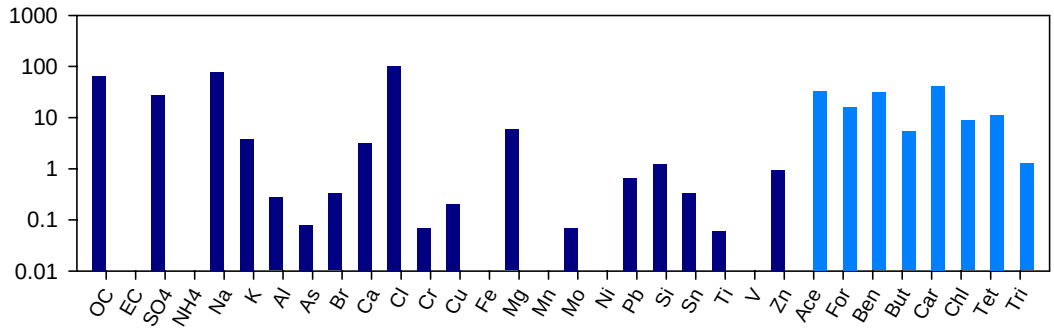

Secondary

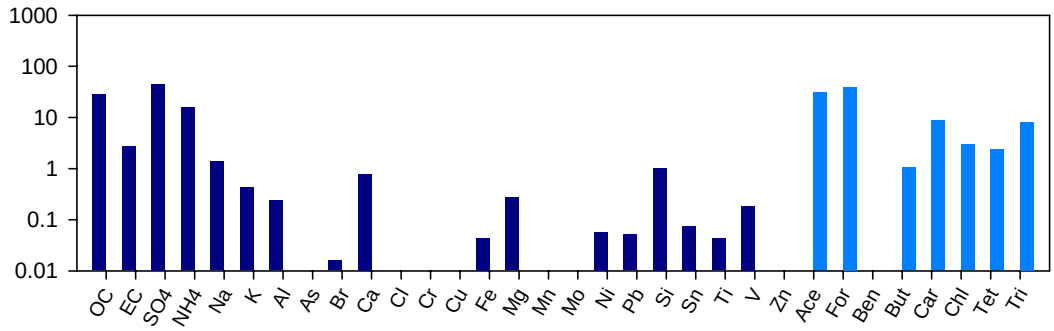

Diesel

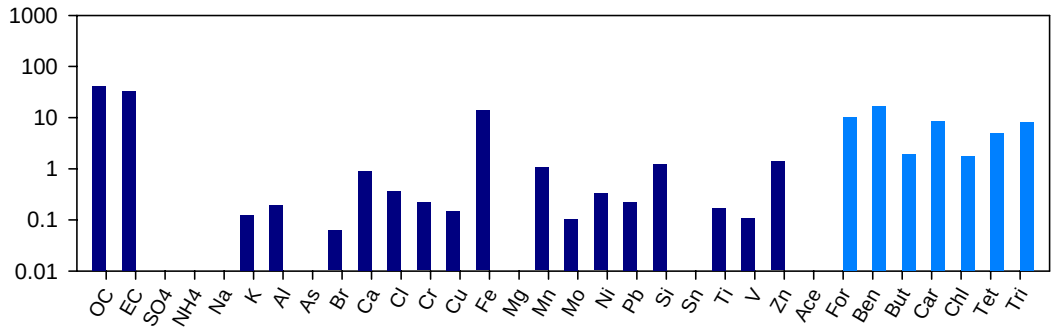

Figure 15. Source features from the PMF model using 24 $PM_{2.5}$ species only at the RL site. (N=252 from 2002.10-2004.12)

Vegetative burning

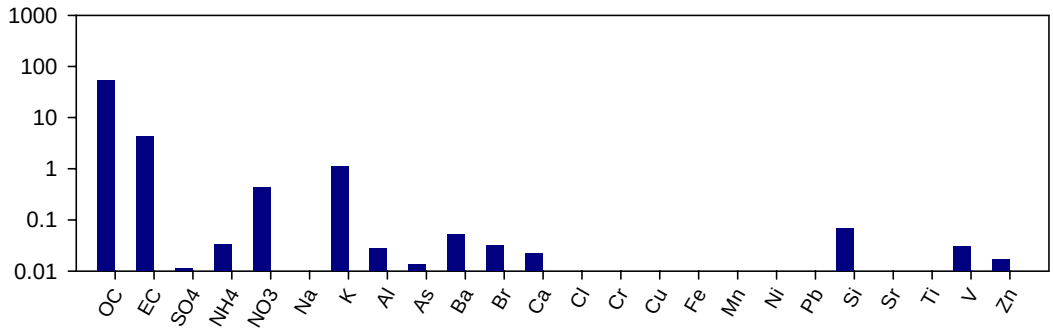

Diesel

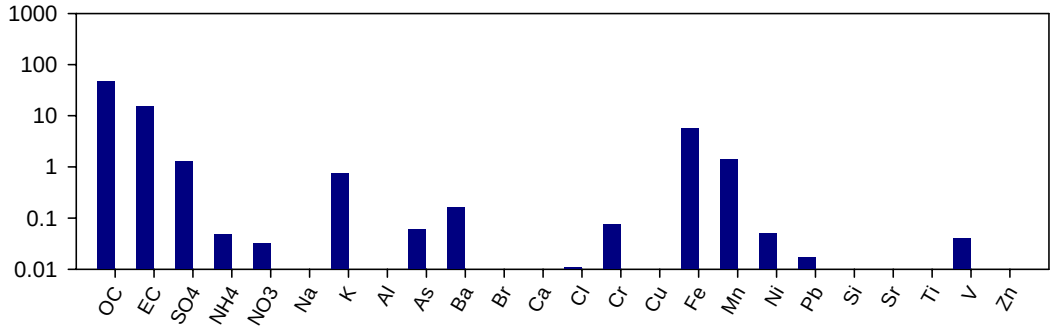

Nitrate rich

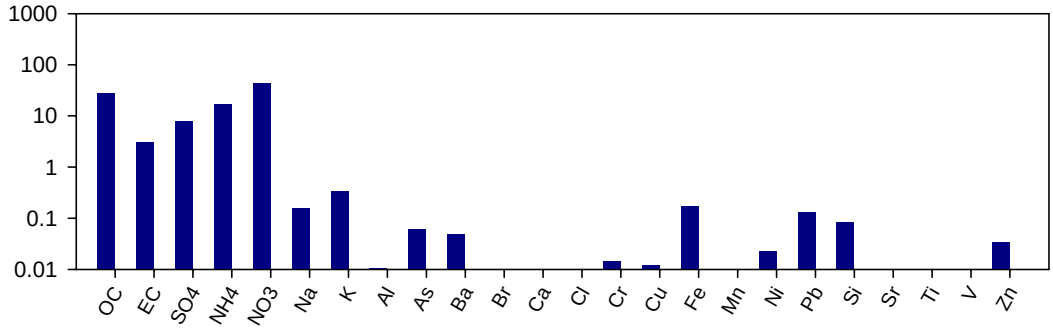

Secondary sulfate

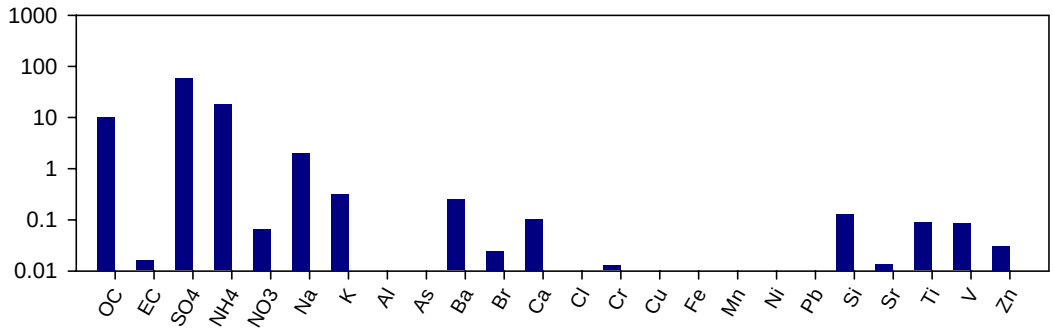

Marine

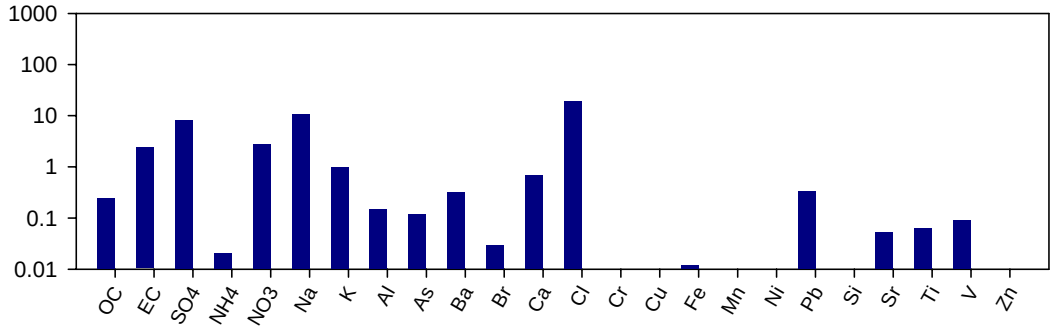

Fuel

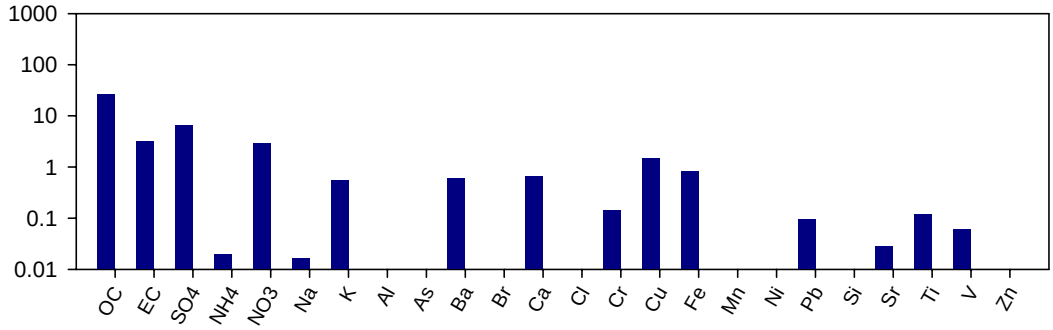

Gasoline

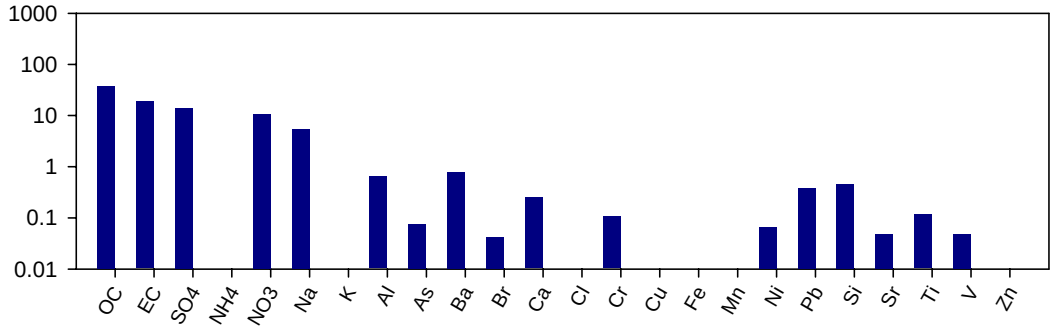

Other 1

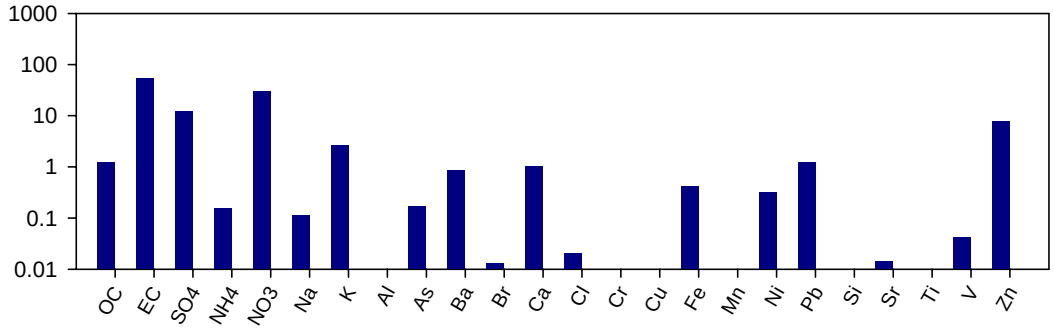

Soil

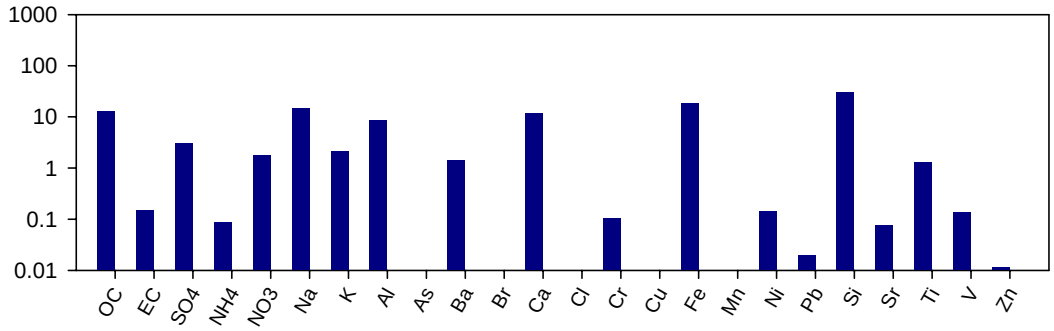

Figure 16. Source contribution estimates (SCE) between heating/non-heating seasons and weekend/weekday form PMF model.

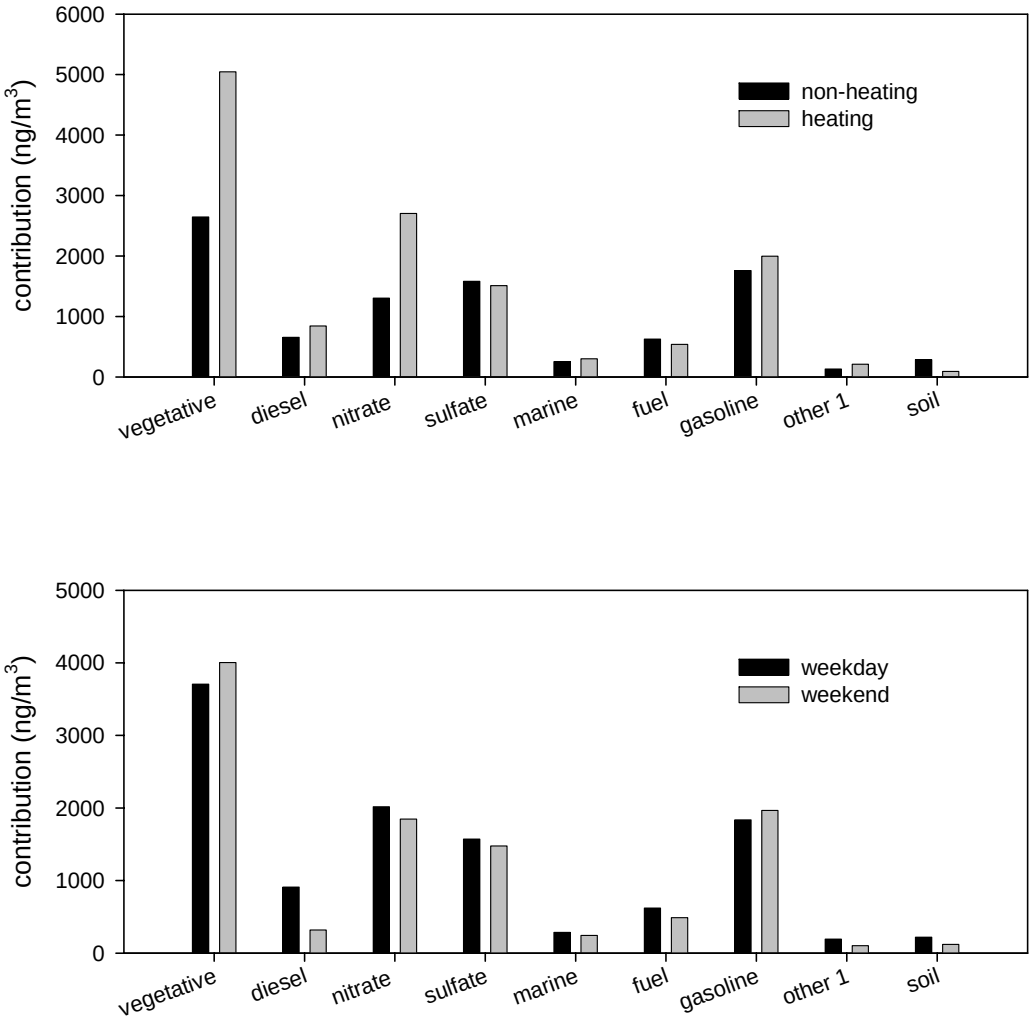

Figure 17. Source features from the ME model using 24 $PM_{2.5}$ species only at the RL site. (N=252 from 2002.10-2004.12)

Fuel

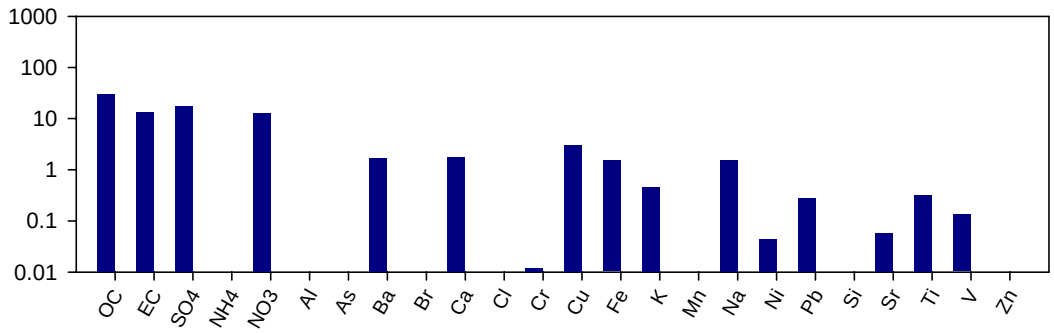

Secondary aerosols

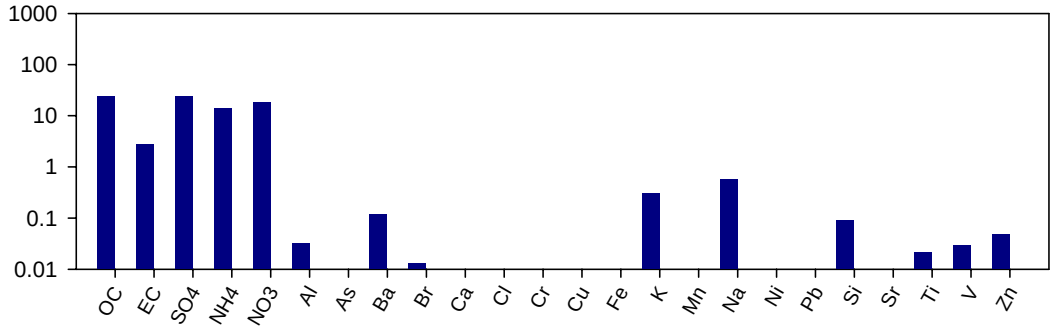

Marine

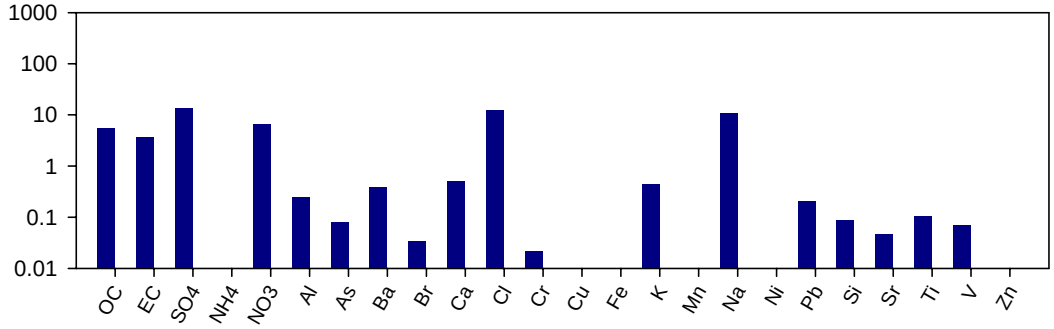

Soil

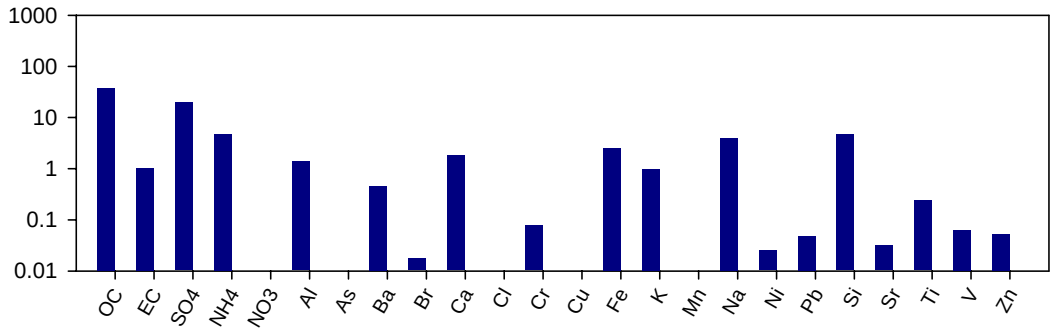

Diesel

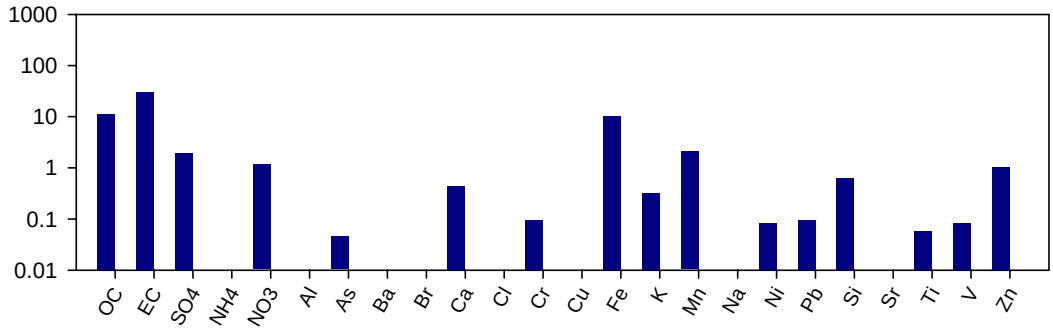

Vegetative burning

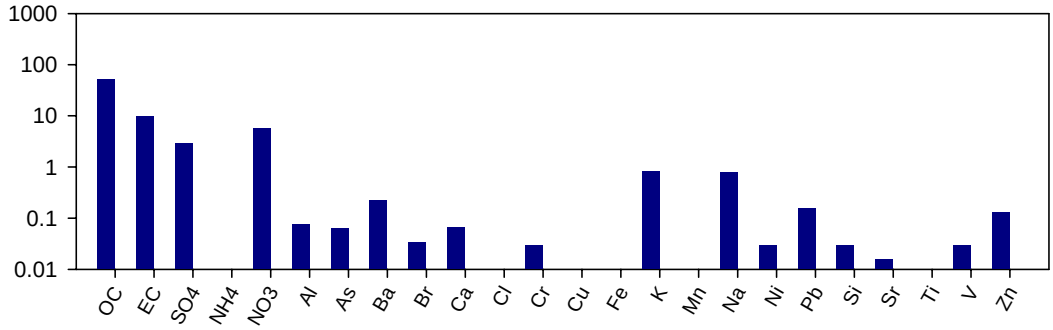

Figure 18. Source contribution estimates (SCE) between heating/non-heating seasons and weekend/weekday form ME model.

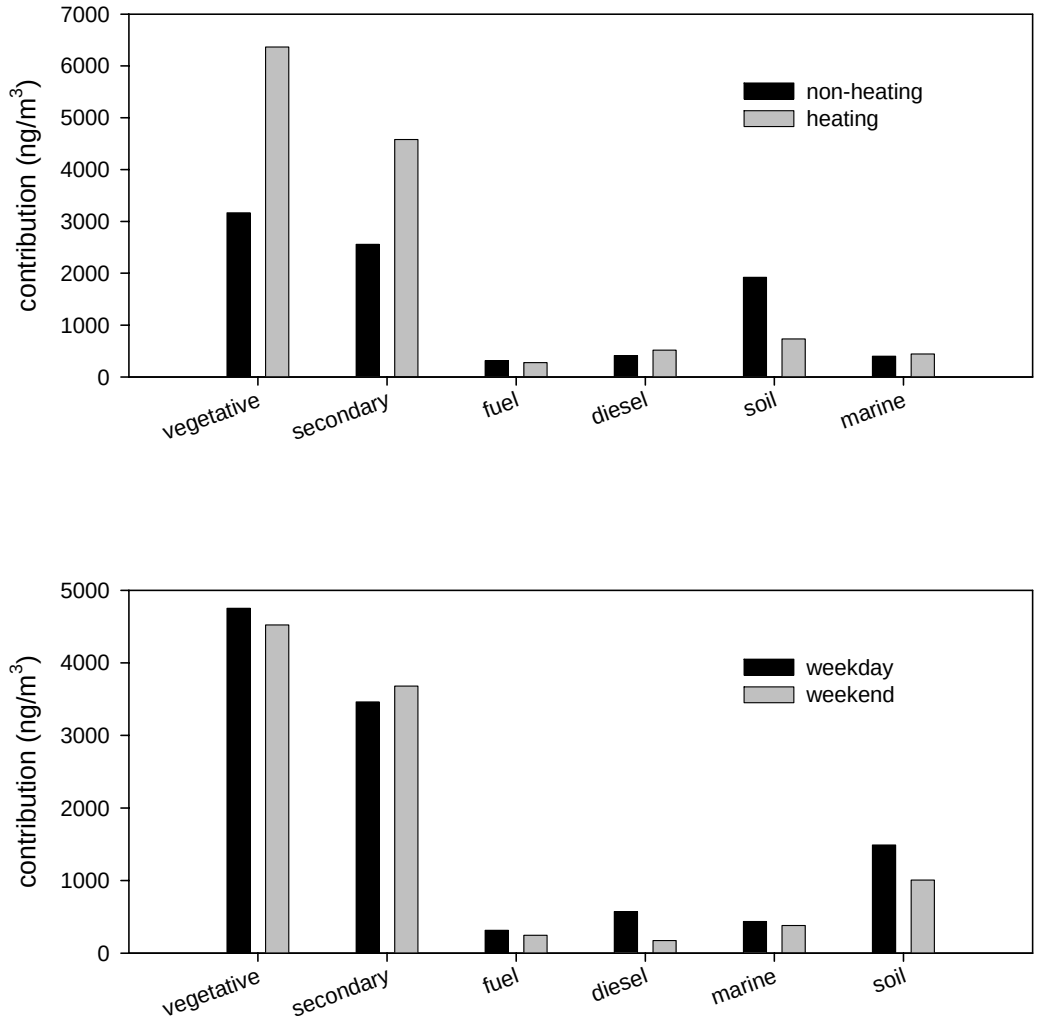

Figure 19. Relationship between the 24-h averaged black carbon (BC) measurements and DPM and BC and vegetative burning PM from the PMF and ME models with the combined $PM_{2.5}$+VOC datasets at Beacon Hill.

(a) BC vs. DPM from PMF during the heating season

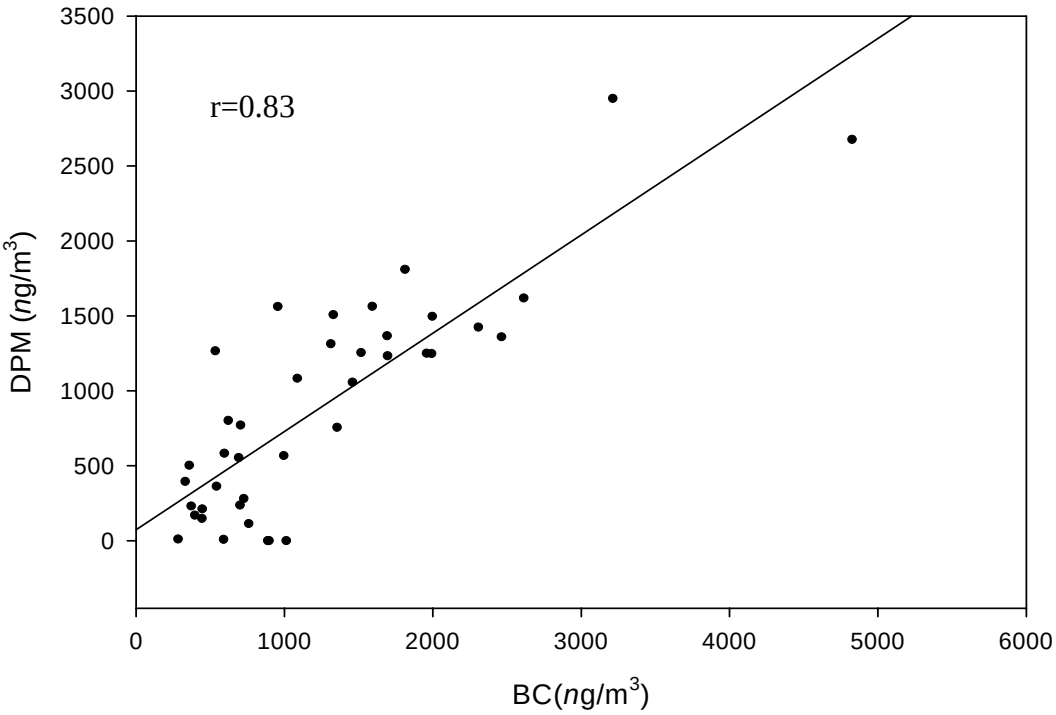

(b) BC vs. DPM from PMF during the non-heating season

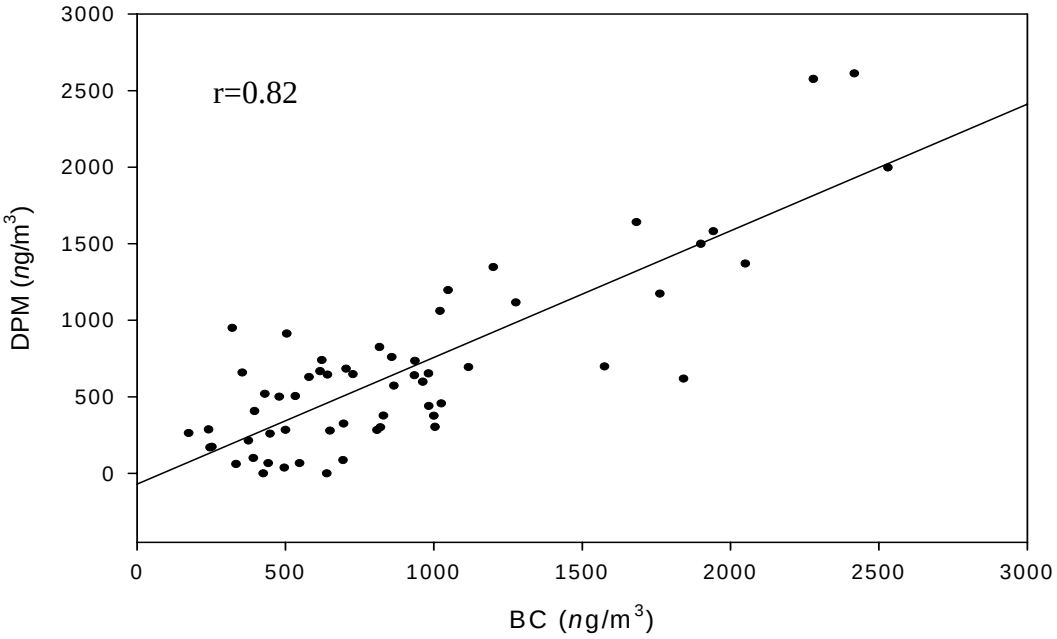

(c) BC vs. vegetative burning from PMF during the heating season

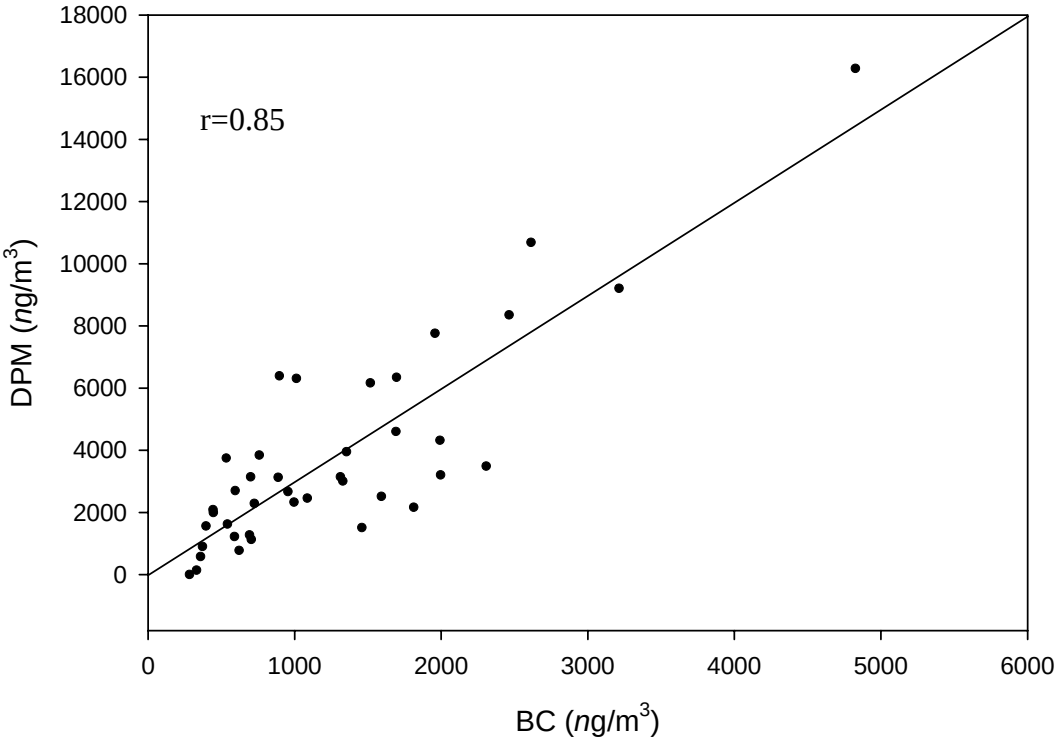

(d) BC vs. vegetative burning from PMF during the non-heating season

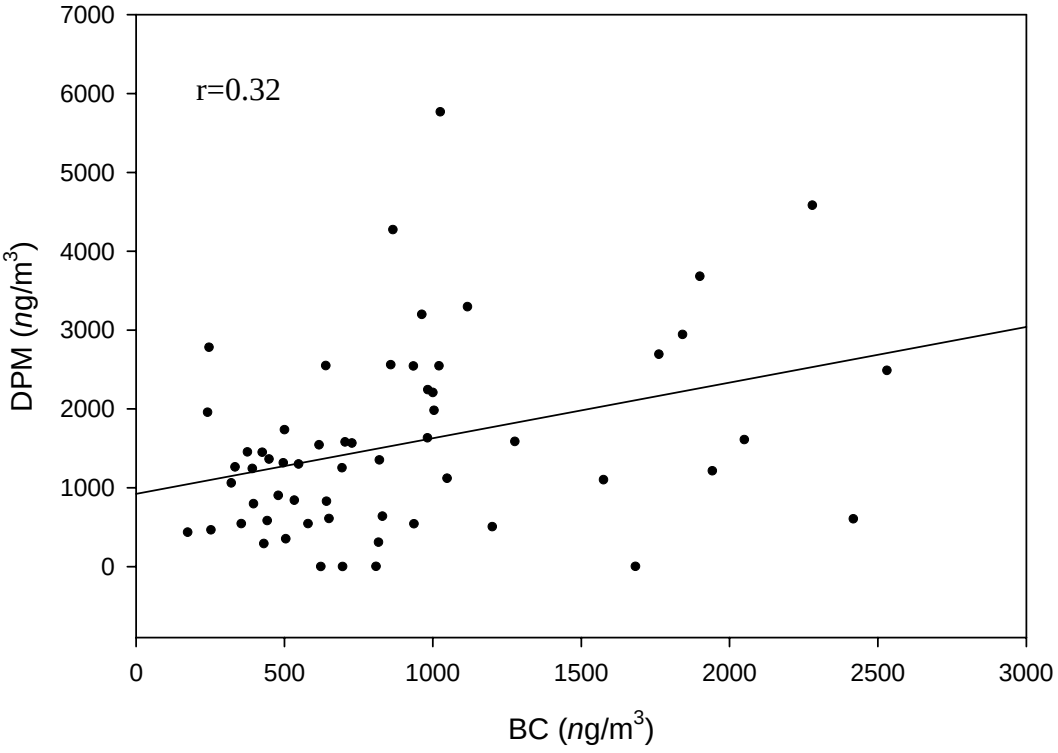

(e) BC vs. DPM from ME during the heating season

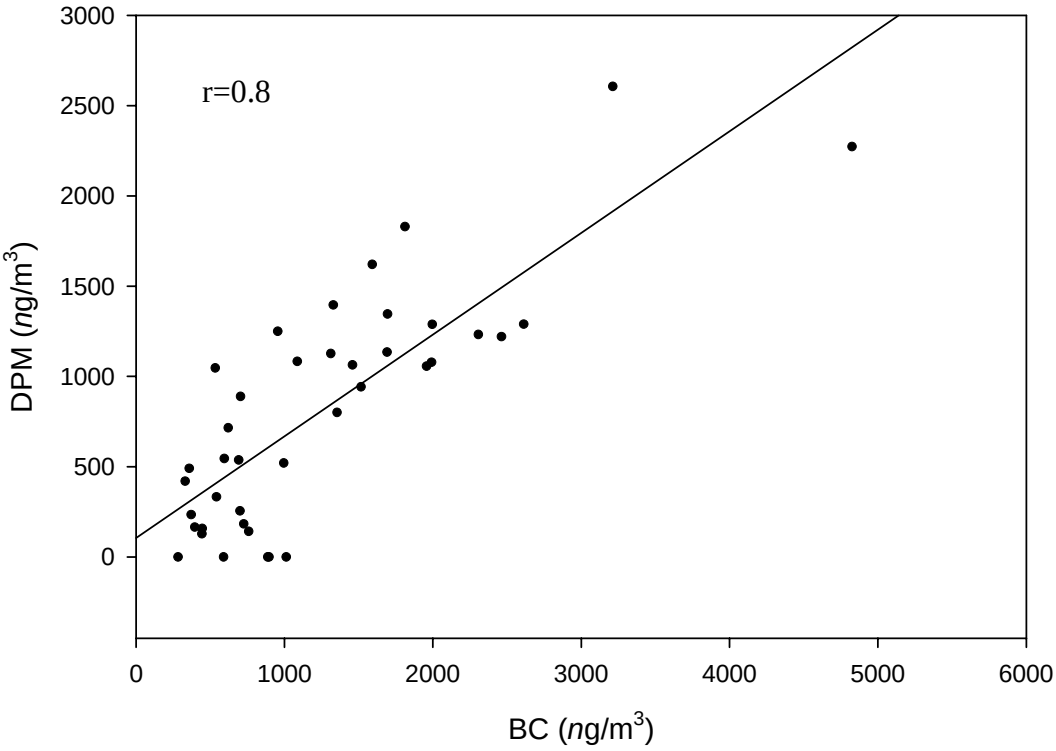

(f) BC vs. DPM from ME during the non-heating season

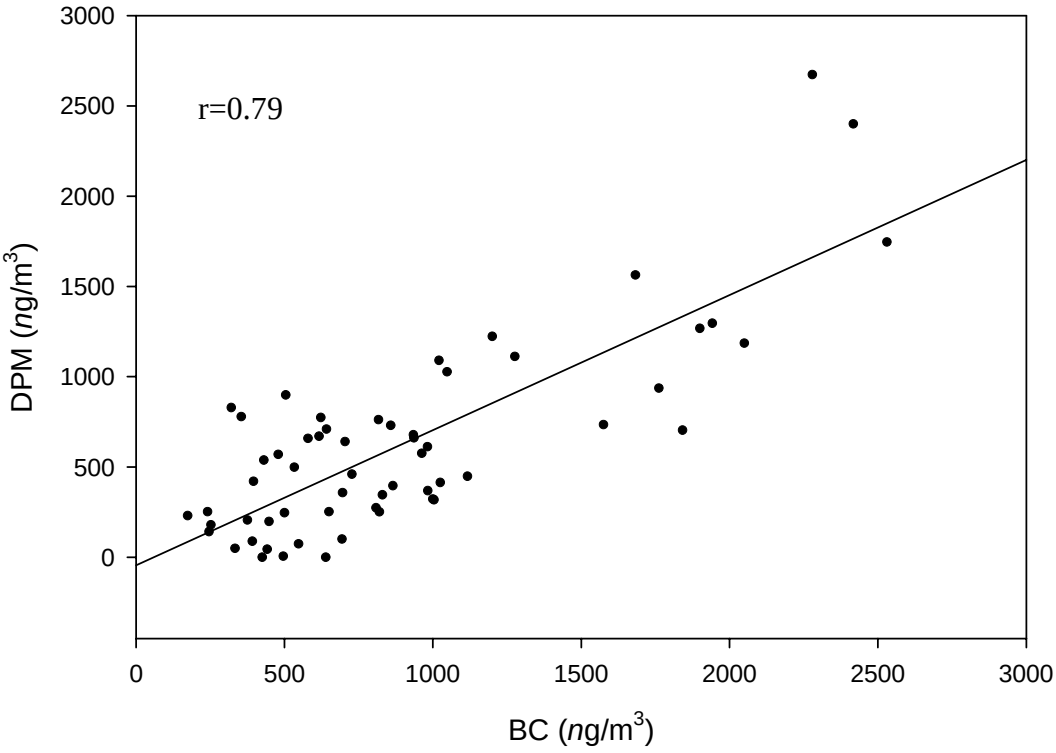

(g) BC vs. vegetative burning from ME during the heating season

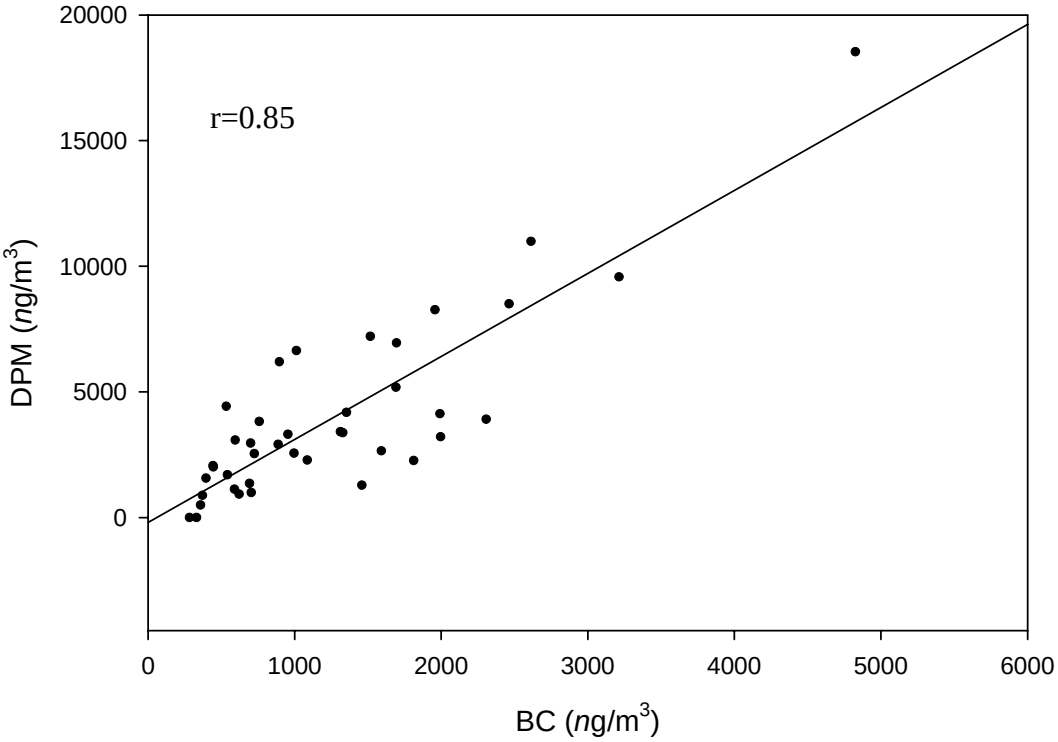

(h) BC vs. vegetative burning from ME during the non-heating season

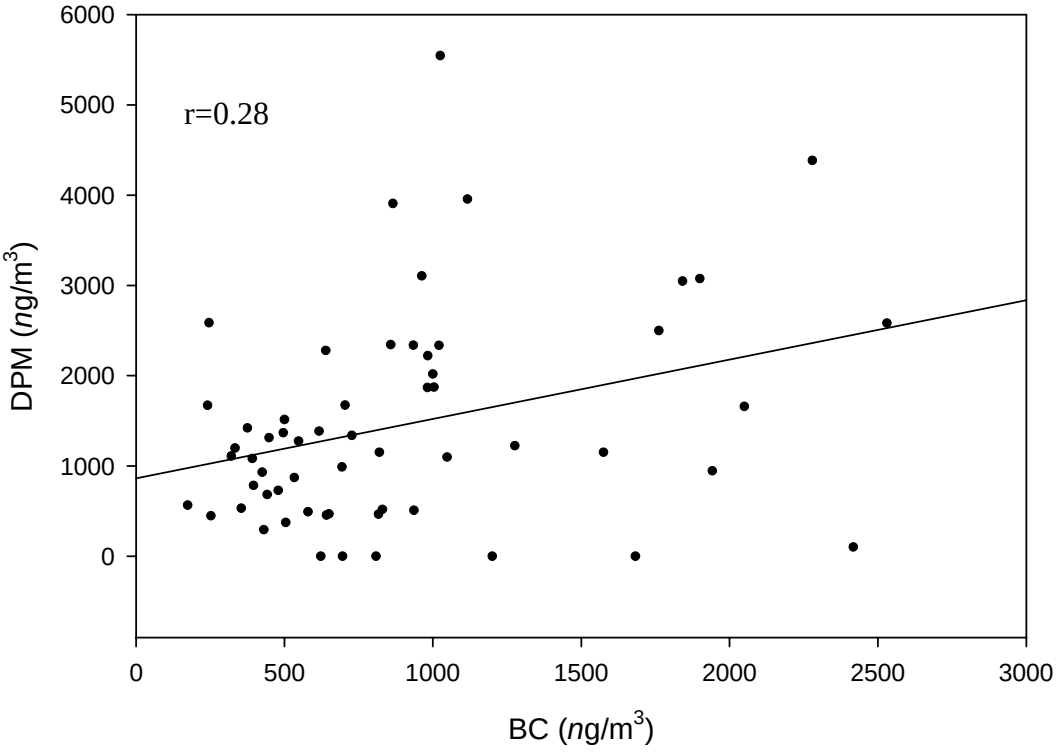

Figure 20. Relationship between the 24-h averaged black carbon (BC) measurements and DPM and BC and vegetative burning PM from the PMF and ME models with $PM_{2.5}$ data only at Beacon Hill.

(a) BC vs. DPM from PMF during the heating season

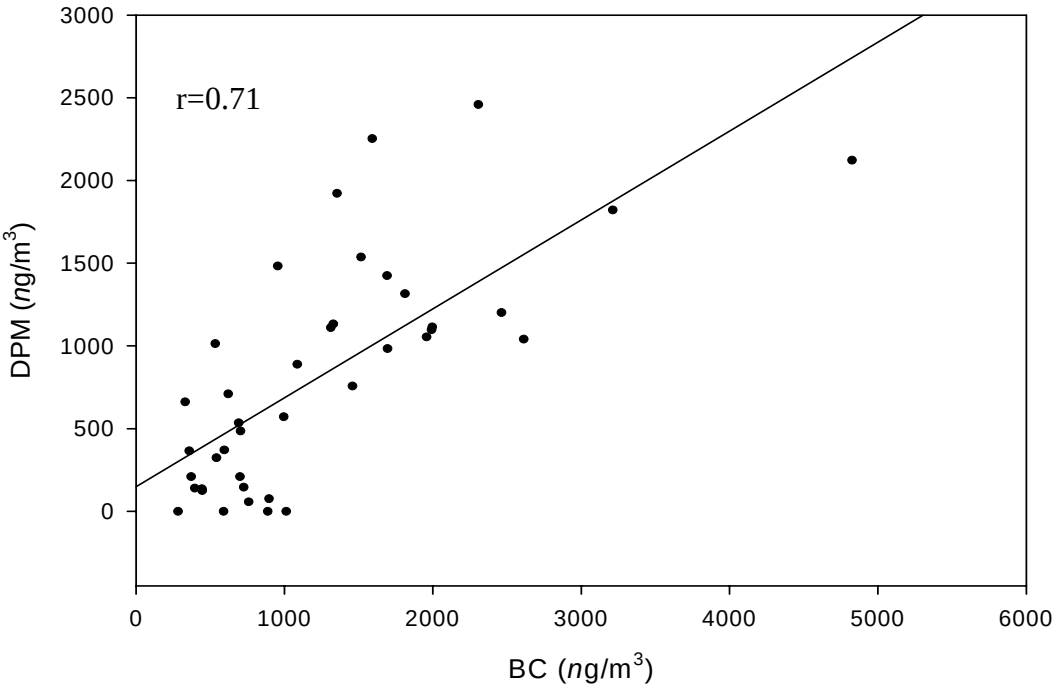

(b) BC vs. DPM from PMF during the non-heating season

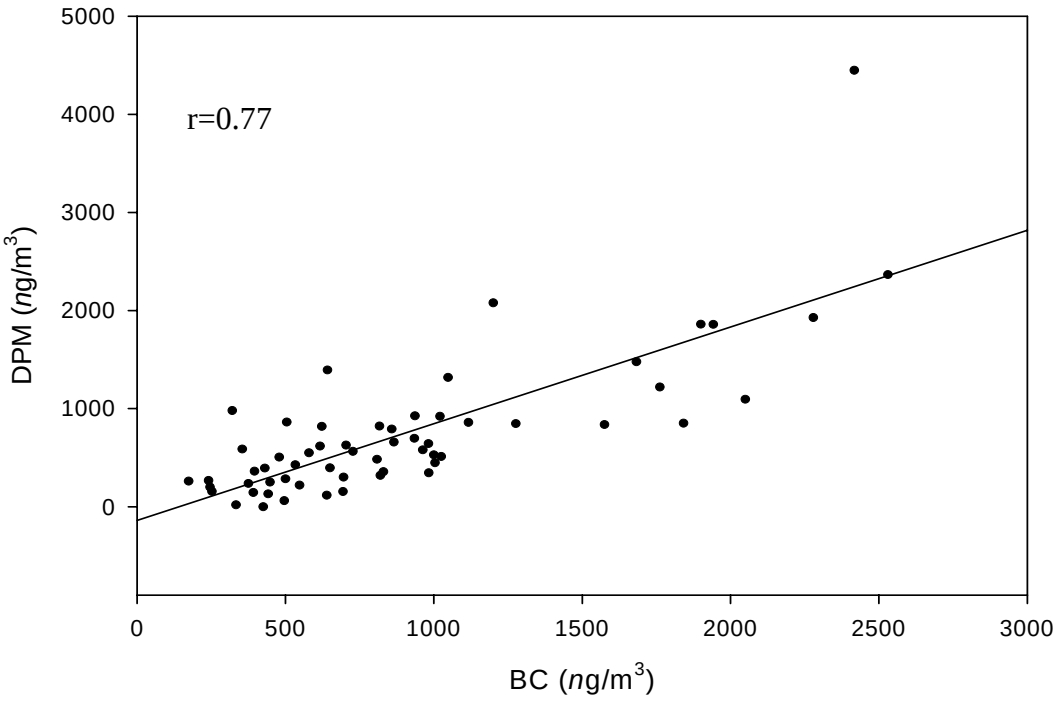

(c) BC vs. vegetative burning from PMF during the heating season

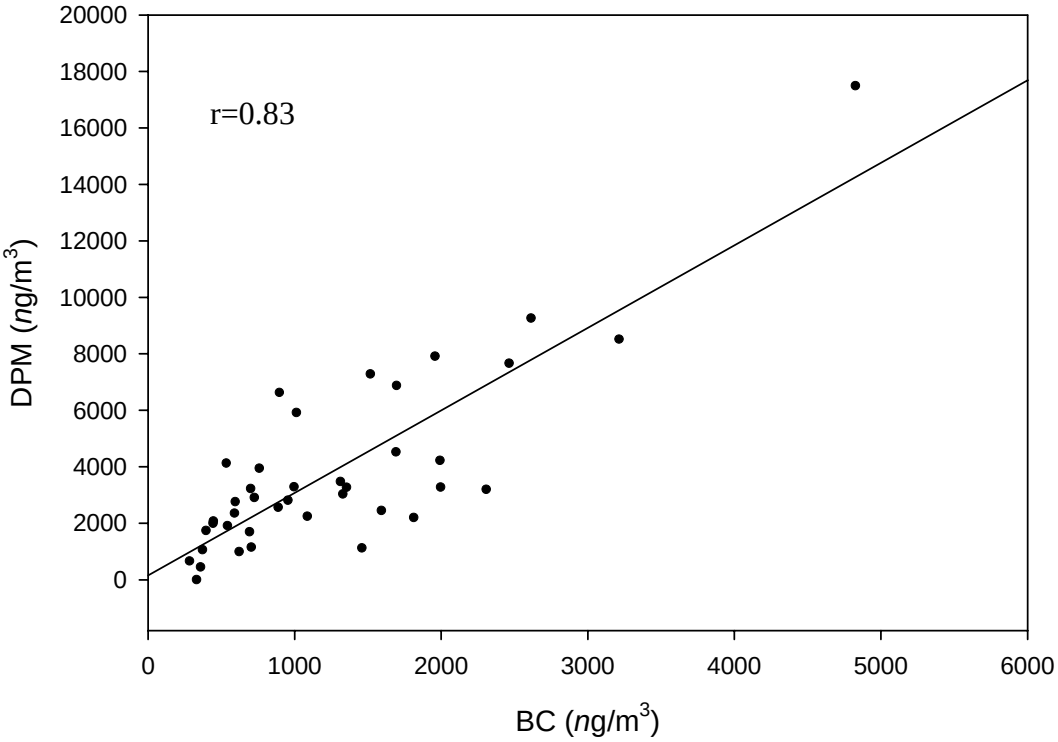

(d) BC vs. vegetative burning from PMF during the non-heating season

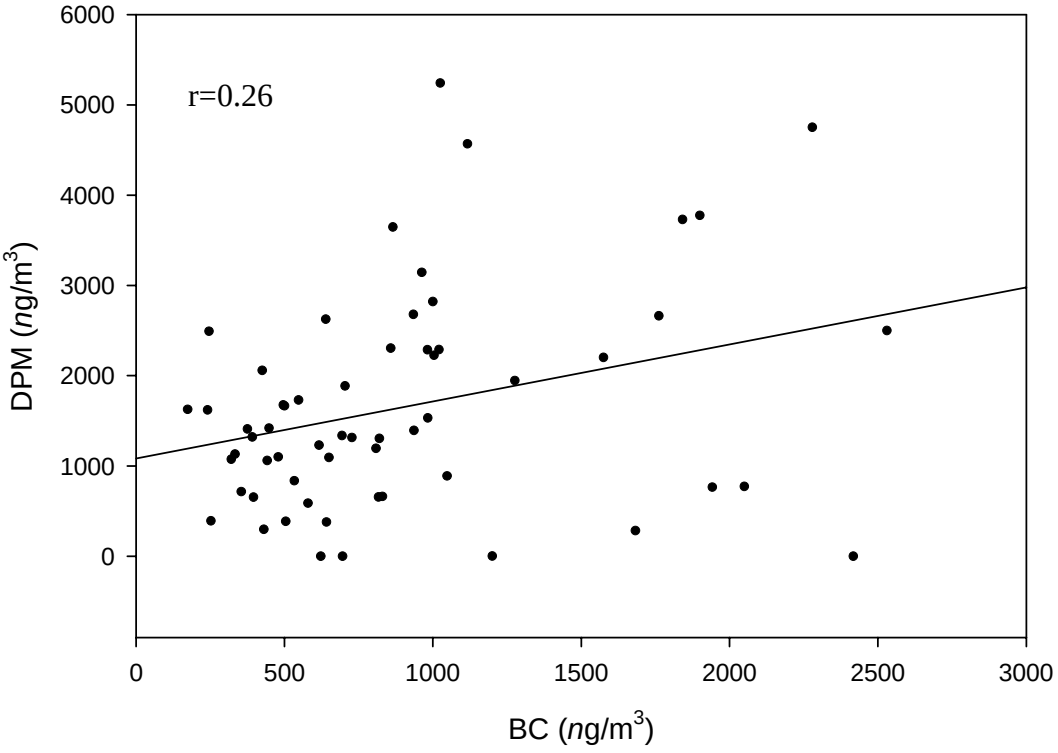

(e) BC vs. DPM from ME during the heating season

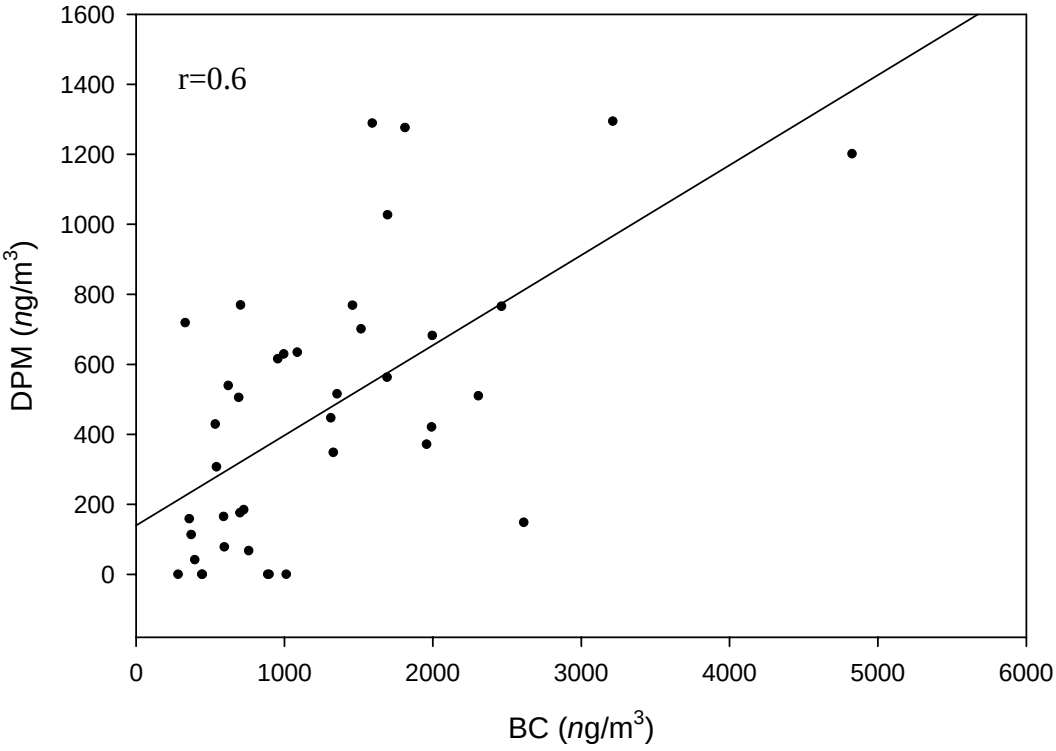

(f) BC vs. DPM from ME during the non-heating season

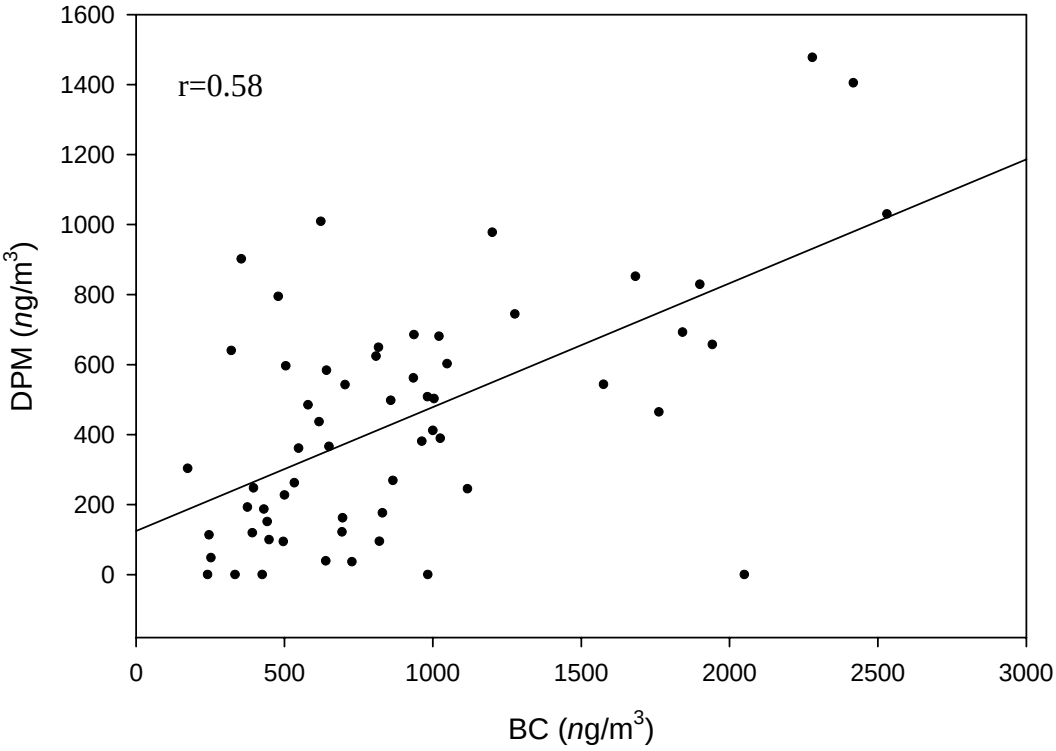

(g) BC vs. vegetative burning from ME during the heating season

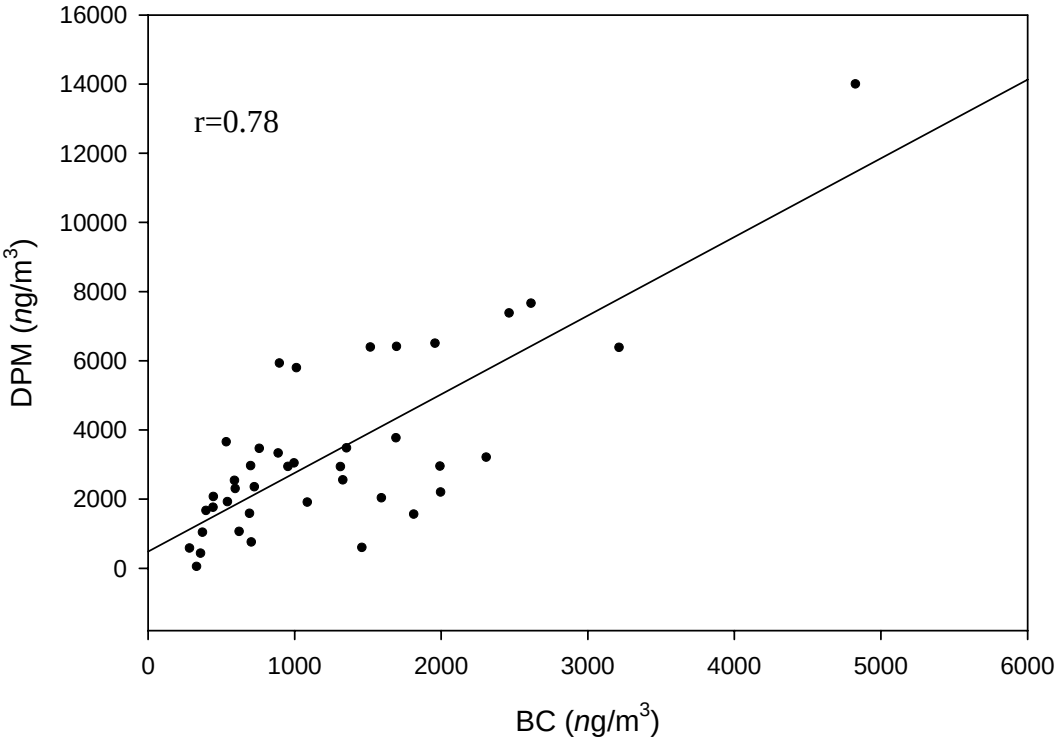

(h) BC vs. vegetative from ME during the non-heating season

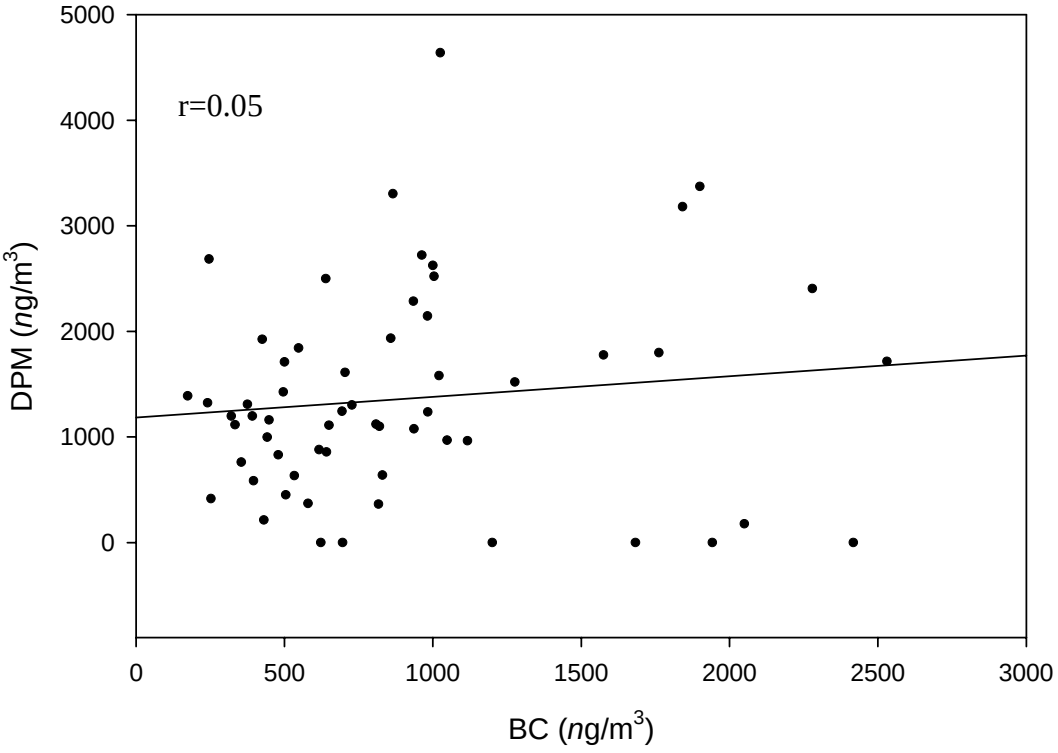

Figure 21. DPM cancer risk estimates from the NATA study using the CalEPA's unit risk.

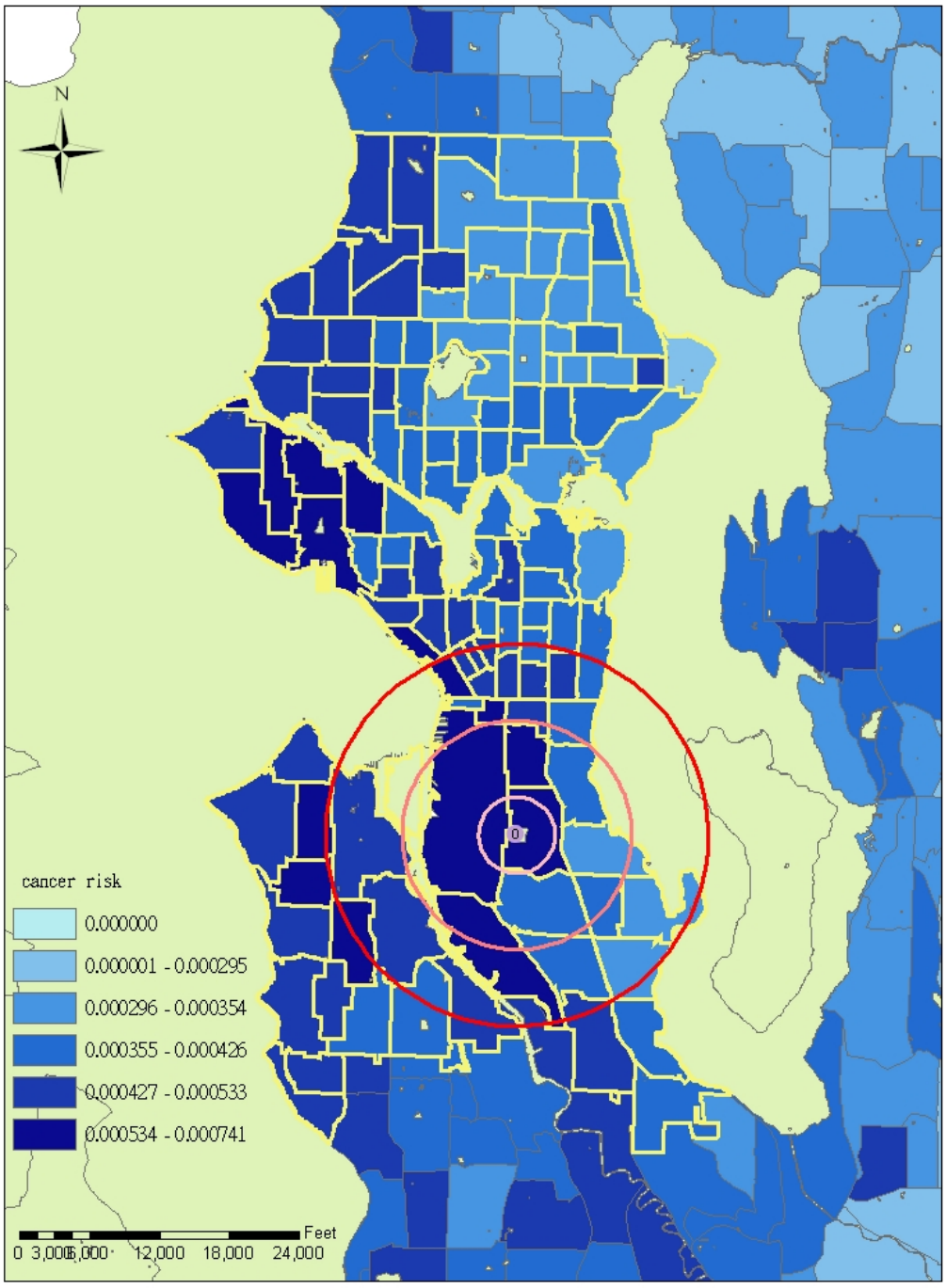

Figure 22. Comparisons of DPM cancer risk estimates at BH from different modeling approaches. PMF(1): Specie-by-specie approach based on DPM source feature from the PMF model using the combined speciated $PM_{2.5}$ and VOC data. PMF(2): DPM concentration estimated from PMF model using the combined speciated $PM_{2.5}$ and VOC data times the CalEPA's unit risk for DPM. NATA(1): Risk estimate from the NATA study at the census tract where the BH site located. NATA(2) ~ NATA (4): Mean risk estimates from the NTAT study at those census tracts falling within 1 km, 3 km, and 5 km from the monitoring site, respectively.